MULTISCALE MODEL. SIMUL.
Vol. 16, No. 1, pp. 385–411

A NEW HETEROGENEOUS MULTISCALE METHOD FOR THE HELMHOLTZ EQUATION WITH HIGH CONTRAST*

MARIO OHLBERGER† AND BARBARA VERFÜRTH†

Abstract. In this paper, we suggest a new heterogeneous multiscale method (HMM) for the Helmholtz equation with high contrast. The method is constructed for a setting as in Bouchitté and Felbacq [*C. R. Math. Acad. Sci. Paris*, 339 (2004), pp. 377–382], where the high contrast in the parameter leads to unusual effective parameters in the homogenized equation. We revisit existing homogenization approaches for this special setting and analyze the stability of the two-scale solution with respect to the wavenumber and the data. This includes a new stability result for solutions to the Helmholtz equation with discontinuous diffusion matrix. The HMM is defined as direct discretization of the two-scale limit equation. With this approach we are able to show quasi-optimality and an a priori error estimate under a resolution condition that inherits its dependence on the wavenumber from the stability constant for the analytical problem. Numerical experiments confirm our theoretical convergence results and examine the resolution condition. Moreover, the numerical simulation gives a good insight and explanation of the physical phenomenon of frequency band gaps.

Key words. multiscale method, finite elements, homogenization, two-scale convergence, Helmholtz equation

AMS subject classifications. 35J05, 35B27, 65N12, 65N15, 65N30, 78M40

DOI. 10.1137/16M1108820

1. Introduction.

The interest in (locally) periodic media, such as photonic crystals, has grown in the last years as they exhibit astonishing properties such as band gaps or negative refraction; see [23, 51, 40]. In this paper, we study *artificial magnetism* in the setting of [11], which has been inspired by the experimental setup of [45].

The electromagnetic properties of a material are governed by the permittivity ε and the permeability μ. Whereas for ε a great range of values can be observed, almost all materials are nonmagnetic, i.e., μ is close to 1. Artificial magnetism now describes the occurrence of an (effective) permeability $\mu_{\text{eff}} \neq 1$ in an originally nonmagnetic material with $\mu = 1$. Clearly, such a material must exhibit some interior structure to allow this significant change of behavior. In [11], an unusual and highly heterogeneous scaling (in the sense of Allaire [2, section 4]) of material parameters (see below) has been used to obtain a frequency-dependent permeability, which can even have a negative real part, in the homogenization limit. The observation that μ_{eff} can even be negative is of particular interest: When ε and μ are negative, such a material can have a negative refraction index, as discussed in [54]. Metals can have a negative real part of ε, but no negative μ can be observed in nature. Moreover, in material with positive ε and negative μ, wave propagation is forbidden, which corresponds to a frequency in the band gap.

The setting of [11], inspired by [45] and [26], is the following (see also Figure 1): A periodic array of rods with high permittivity (depicted in gray in Figure 1) is

*Received by the editors December 20, 2016; accepted for publication (in revised form) November 6, 2017; published electronically March 1, 2018.
http://www.siam.org/journals/mms/16-1/M110882.html
Funding: This work was supported by the Deutsche Forschungsgemeinschaft (DFG) in the project "OH 98/6-1: Wellenausbreitung in periodischen Strukturen und Mechanismen negativer Brechung."
†Angewandte Mathematik: Institut für Analysis und Numerik, Westfälische Wilhelms-Universität Münster, D-48149 Münster (mario.ohlberger@uni-muenster.de, barbara.verfuerth@uni-muenster.de).

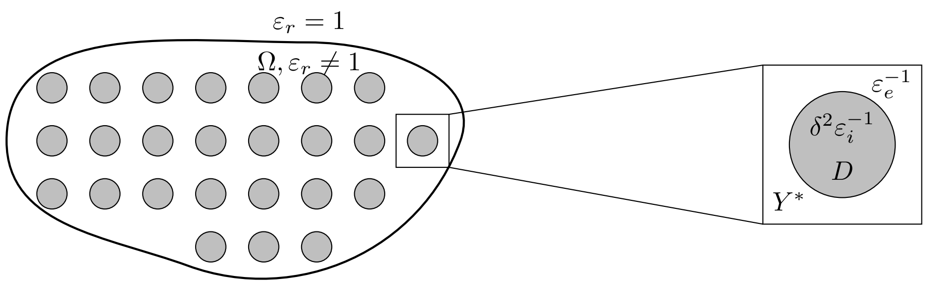

FIG. 1. *Left: Scatterer Ω with highly conductive inclusions D_δ (in gray); Right: Zoom into one unit cell Y and scaling of the permittivity ε_r^{-1}.*

embedded in a lossless dielectric material. Denoting by the small parameter δ the periodicity, the high permittivity in the rods is modeled by setting $\varepsilon^{-1} = \delta^2\varepsilon_i^{-1}$; see section 2 for an exact definition. The consideration of small inclusions with high permittivity has become a popular modeling also in the three-dimensional setting to tune unusual effective material properties; see [10, 12, 13, 17, 38]. Interesting memory effects can occur in the time-dependent setting; see [9].

The overall setting in this paper can be described now as follows: We consider a scatterer of the form $\Omega \times \mathbb{R}$ with $\Omega \subset \mathbb{R}^2$ bounded and smooth (with C^2 boundary). The structure is nonmagnetic, i.e., $\mu = 1$, and has a relative permittivity ε_r, which equals 1 outside Ω. This effectively two-dimensional geometry (invariant in the x_3-direction) is illuminated by a transversely polarized field $\mathbf{H}_{inc} = (0, 0, u_{inc})^T$. The total magnetic field $\mathbf{H} = (0, 0, u)^T$ then satisfies the Helmholtz equation

$$-\nabla \cdot \left(\varepsilon_r^{-1}\nabla u\right) - k^2 u = 0 \quad \text{on} \quad \mathbb{R}^2 \tag{1.1}$$

with the wavenumber $k = \omega/c$. We artificially truncate our domain by introducing a sufficiently large convex Lipschitz domain $G \supset\supset \Omega$ and imposing on ∂G the following boundary condition

$$\nabla u \cdot n - iku = g := \nabla u_{inc} \cdot n - iku_{inc}, \tag{1.2}$$

which is the popular first order approximation of the Sommerfeld radiation condition; cf. [19, 36]. The relative permittivity $\varepsilon_r = a_\delta^{-1}$ inside the scatterer models the described setting of periodic inclusions with high permittivity and is defined in (2.2). Throughout this article, we assume that there is $k_0 > 0$ such that $k \geq k_0$, which corresponds to medium and high frequencies.

A numerical treatment of (1.1) with boundary condition (1.2) and permittivity with high contrast is very challenging. Solutions to Helmholtz problems show oscillatory behavior in general and the consideration of (locally) periodic media intensifies this effect. The challenge is then to well approximate the heterogeneities in the material and the oscillations induced by the incoming wave. It is important to relate the scales of these oscillations: We basically have a three-scale structure here with $\delta \ll k^{-1} < 1$, i.e., the periodicity of the material (and the size of the inclusions) is much smaller than the wavelength of the incoming wave. A direct discretization requires a grid with mesh size $h < \delta \ll 1$ to approximate the solution faithfully. This can easily exceed today's computational resources when using a standard approach. In order to make a numerical simulation feasible, so-called multiscale methods can be applied. The family of heterogeneous multiscale methods (HMM) [20, 21] is a class of multiscale methods that has been proved to be very efficient for scale-separated locally periodic problems. The HMM can exploit local periodicity in the coefficients to solve local sample problems that allow one to extract effective macroscopic features and to approximate solutions with a complexity independent of the (small) periodicity δ. First analytical results concerning the approximation properties of the HMM for elliptic problems have been derived in [1, 22, 29, 46] and then extended to other problems, such as time-harmonic Maxwell's equations [32]. Other related works are the HMM for Helmholtz problems with locally periodic media (without high contrast!) [18], or a multiscale asymptotic expansion for the Helmholtz equation [15]. The HMM itself can also be applied to nonperiodic settings; see [29, 31]. However, it is by no means clear whether the (analytical) setting under consideration in this paper has a meaningful extension beyond the (locally) periodic case.

The new contribution of this article is the first formulation of an HMM for the Helmholtz equation with high contrast in the setting of [11], its comprehensive numerical analysis and its implementation. The numerical experiment not only shows the practicality of the suggested HMM, but also gives an enlightening insight into the physical background of artificial magnetism and frequency band gaps. The HMM can be used to approximate the true solution to (1.1) with a much coarser mesh and hence less computational effort. We observe that for a frequency in the band gap, wave propagation is prohibited due to destructive interference of waves incited at eigen resonances of the small inclusions with high permittivity. From the theoretical point of view, the main result is that the energy error converges with rate $k^{q+1}(H+h)$ if the resolution condition $k^{q+2}(H+h)=O(1)$ is fulfilled. Here, H and h denote the δ-independent mesh sizes used for the HMM and we assume that the analytical two-scale solution has a stability constant of order k^q with $q\in\mathbb{N}_0$. This resolution condition is unavoidable for standard Galerkin discretizations of Helmholtz problems and it shows up with $q=0$ (the optimal case) in our numerical experiments. A posteriori estimates in this setting are equally possible to obtain. The described HMM itself might be transferable/adaptable to similarly scaled situations in three dimensions.

To complement our numerical analysis, we also show an explicit stability estimate for the solution to the two-scale limit equation, so that we have an explicit (though maybe suboptimal) result for the stability exponent $q=3$. This includes a second contribution, which may be of its own interest: A new stability result for a certain class of Helmholtz-type problems, namely, with matrix-valued discontinuous diffusion coefficient. Stability results for the Helmholtz equation have only been proved in the following cases: Constant coefficients have been studied under various geometrical conditions in [5, 24, 33, 41, 42, 43] and scalar-valued, globally Lipschitz continuous coefficients have been treated in [14]. Only recently (during the review process of this paper), has a detailed stability analysis of the Helmholtz equation with scalar-valued, discontinuous coefficients been conducted in [44].

The article is organized as follows: In section 2 we detail the (geometric) setting of the heterogeneous problem considered and give some basic notation used throughout the article. We present and combine existing homogenization results and analyze the homogenized problems in detail in section 3. This is the motivation and starting point for the formulation of the corresponding HMM in section 4. The quasi-optimality and a priori estimates for the new method as the central statement of the article are given in section 5. All essential proofs are detailed in section 6. A numerical experiment is presented in section 7.

2. Problem setting. For the remainder of this article, let $\Omega \subset\subset G \subset \mathbb{R}^2$ be two bounded domains, where $\partial\Omega$ is of class C^2 and G is convex and has a polygonal Lipschitz boundary. Throughout this paper, we use standard notation: For a domain ω, $p \in [1, \infty)$ and $s \in \mathbb{R}_{\geq 0}$, $L^p(\omega)$ denotes the usual complex Lebesgue space with norm $\|\cdot\|_{L^p(\omega)}$ and $H^s(\omega)$ denotes the complex (fractional) Sobolev space with the norm $\|\cdot\|_{H^s(\omega)}$. The domain ω is omitted from the norms if no confusion can arise. The dot will denote a normal (real) scalar product, for a complex scalar product we will explicitly conjugate the second component by using v^* as the conjugate complex of v. The L^2 scalar product on a domain ω is abbreviated by $(\cdot,\cdot)_\omega$ and the corresponding norm abbreviated by $\|\cdot\|_\omega$. For a polygonally bounded domain ω, $H^{1/2}(\partial\omega)$ denotes the space of functions which are edgewise $H^{1/2}$. For the domain G, we abbreviate by

$$H^s_{pw}(G) := H^s(\Omega) \cap H^s(G \setminus \overline{\Omega}) \cap H^1(G), \quad s > 1, \tag{2.1}$$

the function space of piecewise H^s functions and note that $H^s_{pw}(G) = H^s(G)$ for $s \in [1, \frac{3}{2})$; see [50]. For $v \in H^1(\omega)$, we frequently use the k-dependent norm

$$\|v\|_{1,k,\omega} := \left(\|\nabla v\|^2_\omega + k^2\|v\|^2_\omega\right)^{1/2},$$

which is obviously equivalent to the H^1-norm.

Let $\mathbf{e}_j$ denote the jth unit vector in $\mathbb{R}^2$. For the rest of the paper, we write $Y := [-\frac{1}{2}, \frac{1}{2})^2$ to denote the two-dimensional unit square and we say that a function $v \in L^2_{loc}(\mathbb{R}^2)$ is Y-periodic if it fulfills $v(y) = v(y+\mathbf{e}_j)$ for all $j = 1, 2$ and almost every $y \in \mathbb{R}^2$. With that we denote $L^2_\sharp(Y) := \{v \in L^2_{loc}(\mathbb{R}^2) | v \text{ is } Y\text{-periodic}\}$. Analogously we indicate periodic function spaces by the subscript $\sharp$. For example, $H^1_\sharp(Y)$ is the space of periodic $H^1_{loc}(\mathbb{R}^2)$ functions and we define

$$H^1_{\sharp,0}(Y) := \left\{\phi \in H^1_\sharp(Y) \middle| \int_Y \phi = 0\right\}.$$

For $Y^* \subset Y$, we denote by $H^1_{\sharp,0}(Y^*)$ the restriction of functions in $H^1_{\sharp,0}(Y)$ to Y^*. For $D \subset\subset Y$, $H^1_0(D)$ can be interpreted as a subspace of $H^1_\sharp(Y)$ and we will write $H^1_0(D)_\sharp$ to emphasize this periodic extension. By $L^p(\Omega; X)$ we denote Bochner–Lebesgue spaces over the Banach space X and we use the short notation $f(x, y) := f(x)(y)$ for $f \in L^p(\Omega; X)$. Functions in $L^2(\Omega)$ are also regarded as functions in $L^2(G)$ by simple extension by zero.

Using the above notation we consider the following setting for the (inverse) relative permittivity ε_r^{-1}; see [11]: Ω is composed of δ-periodically-disposed sections of rods, δ being a small parameter. Denoting by $D \subset\subset Y$ a connected domain with C^2 boundary, the rods occupy a region $D_\delta := \cup_{j\in I}\delta(j+D)$ with $I = \{j \in \mathbb{Z}^2 | \delta(j+Y) \subset \Omega\}$. The complement of D in Y, which is also connected, is denoted by Y^*. The inverse relative permittivity $a_\delta := \varepsilon_r^{-1}$ is then defined (possibly after rescaling) as (cf. Figure 1)

$$a_\delta(x) := \begin{cases} \delta^2\varepsilon_i^{-1} & \text{if } x \in D_\delta \qquad \text{with } \varepsilon_i \in \mathbb{C}, \operatorname{Im}(\varepsilon_i) > 0, \operatorname{Re}(\varepsilon_i) > 0, \\ \varepsilon_e^{-1} & \text{if } x \in \Omega \setminus D_\delta \qquad \text{with } \varepsilon_e \in \mathbb{R}_+, \\ 1 & \text{if } x \in G \setminus \overline{\Omega}. \end{cases} \tag{2.2}$$

We assume $\operatorname{Re}(\varepsilon_i) > 0$ for simplicity; all results hold—up to minor modifications in the proofs; also for ε_i with $\operatorname{Re}(\varepsilon_i) \leq 0$. Physically speaking, this means that the scatterer Ω consists of periodically disposed metallic rods D_δ embedded in a dielectric "matrix" medium. The scaling of δ^2 in the rods corresponds to a constant optical diameter of these inclusions.

It is essential that $\Omega \backslash D_\delta$ is connected, otherwise the two-scale convergences shown below can fail; see [13] for an example. To assume D as connected is only done for simplicity.

DEFINITION 2.1 (weak solution). *Let the parameter a_δ be defined by* (2.2) *and let $g \in H^{1/2}(\partial G)$. We call $u_\delta \in H^1(G)$ a weak solution if it fulfills*

$$\int_G a_\delta(x)\nabla u_\delta \cdot \nabla \psi^* - k^2 u_\delta \psi^* \, dx - ik \int_{\partial G} u_\delta \psi^* \, d\sigma = \int_{\partial G} g\psi^* \, d\sigma \quad \forall \psi \in H^1(G). \tag{2.3}$$

It is well known that for fixed δ, there is a unique solution to (2.3), which can be seen using the Fredholm alternative: The left-hand side fulfills a Gårding inequality and problem (2.3) as well as the adjoint problem are uniquely solvable. Throughout the article, C denotes a generic constant, which does not depend on k (and later the mesh sizes H and h), but may depend on k_0 and may vary from line to line.

3. Homogenization and analysis of the homogenized equations. As the parameter δ is assumed to be very small in comparison to the wavelength and the typical length scale of Ω, one can reduce the complexity of problem (2.3) by considering the limit $\delta \to 0$. This process, called homogenization, can be performed with the tool of two-scale convergence [2, 39] for locally periodic problems. In subsection 3.1, we adopt the two-scale equation from [2, section 4], derived for highly heterogeneous diffusion problems with Dirichlet boundary condition, and the homogenized effective macroscopic equation from [11] (with Sommerfeld radiation condition) to our setting. Subsection 3.2 is devoted to a detailed analysis of the two-scale equation and its homogenized formulation. Most importantly, this subsection includes a new stability result for solutions to Helmholtz-type problems, generalizing results available in the literature to a larger class of coefficients. We emphasize that this analysis is an important building block and prerequisite for the numerical analysis in section 4.

3.1. Two-scale equation and homogenized formulation. Two-scale convergence is a special form of convergence for locally periodic functions, which tries to capture oscillations and lies between weak and strong (norm) convergence. Its definition and main properties can be found in [2] or [39], for instance. We write $\overset{2}{\rightharpoonup}$ for the two-scale convergence in short form.

The special scaling of a_δ with δ^2 on a part of Ω leads to a different behavior of the solution on D_δ and its complement, which can still be seen in the two-scale equation and the homogenized (effective) equation.

THEOREM 3.1 (two-scale equation). *Let u_δ be the weak solution to* (2.3). *There are functions $u \in H^1(G)$, $u_1 \in L^2(\Omega; H^1_{\sharp,0}(Y^*))$, and $u_2 \in L^2(\Omega; H^1_0(D)_\sharp)$ such that we have the following two-scale convergences for $\delta \to 0$:*

$$\begin{aligned} u_\delta &\overset{2}{\rightharpoonup} u(x) + \chi_D(y)u_2(x,y), & \chi_{\Omega\backslash\overline{D}_\delta}\nabla u_\delta &\overset{2}{\rightharpoonup} \chi_{Y^*}(y)(\nabla u(x) + \nabla_y u_1(x,y)), \\ \delta\chi_{D_\delta}\nabla u_\delta &\overset{2}{\rightharpoonup} \chi_D(y)\nabla_y u_2(x,y), & \nabla u_\delta &\overset{2}{\rightharpoonup} \nabla u \quad \text{in} \quad G \setminus \overline{\Omega}. \end{aligned}$$

Here, the two-scale triple $\mathbf{u} := (u, u_1, u_2)$ *is the unique solution of*

(3.1)

$$\mathcal{B}((u, u_1, u_2), (\psi, \psi_1, \psi_2)) = \int_{\partial G} g\psi^* \, d\sigma,$$
$$\forall \boldsymbol{\psi} := (\psi, \psi_1, \psi_2) \in H^1(G) \times L^2\left(\Omega; H^1_{\sharp,0}(Y^*)\right) \times L^2\left(\Omega; H^1_0(D)_\sharp\right)$$

with the two-scale sesquilinear form $\mathcal{B}$ *defined by*

$$\begin{aligned}\mathcal{B}(\mathbf{v}, \boldsymbol{\psi})&\\ := \int_\Omega \int_{Y^*} \varepsilon_e^{-1}(\nabla v + \nabla_y v_1) \cdot (\nabla \psi^* + \nabla_y \psi_1^*) \, dydx + \int_\Omega \int_D \varepsilon_i^{-1} \nabla_y v_2 \cdot \nabla_y \psi_2^* \, dydx&\\ - k^2 \int_G \int_Y (v + \chi_D v_2)(\psi^* + \chi_D \psi_2^*) \, dydx + \int_{G \setminus \overline{\Omega}} \nabla v \cdot \nabla \psi^* \, dx - ik \int_{\partial G} v\psi^* \, d\sigma.&\end{aligned}$$

The proof mainly follows the lines of [11] with the application of the two-scale convergences proved in [2, section 4] for a highly heterogeneous diffusion problem. Note that u_1 and u_2 are zero outside Ω so that we have $u_\delta \rightharpoonup u$ in $H^1(G \setminus \overline{\Omega})$. We remark that the two-scale equation for a problem with highly heterogeneous coefficients includes two correctors and especially a corrector in the identity part—in contrast to the classical elliptic case; see [2, 39].

The two-scale equation can be recast into a homogenized macroscopic equation which involves effective parameters computed from cell problems, as given in the next theorem.

THEOREM 3.2 (homogenized macroscopic equation). (u, u_1, u_2) *solves the two-scale equation* (3.1) *if and only if we set* $u_1(x, y) = \sum_{j=1}^2 \frac{\partial u}{\partial x_i}|_\Omega(x) w_j(y)$, $u_2(x, y) = k^2 u|_\Omega(x) w(y)$, *and* $u \in H^1(G)$ *solves*

$$B_{\text{eff}}(u, \psi) = \int_{\partial G} g\psi^* \, d\sigma \qquad \forall \psi \in H^1(G) \tag{3.2}$$

with the effective sesquilinear form

$$B_{\text{eff}}(v, \psi) := \int_G a_{\text{eff}} \nabla v \cdot \nabla \psi^* - k^2 \mu_{\text{eff}} v \psi^* \, dx - ik \int_{\partial G} v\psi^* \, d\sigma. \tag{3.3}$$

Here, the effective parameters are defined as

$$(a_{\text{eff}}(x))_{jk} := \begin{cases} \int_{Y^*} \varepsilon_e^{-1}(\mathbf{e}_j + \nabla_y w_j) \cdot (\mathbf{e}_k + \nabla_y w_k^*) \, dy & \text{if } x \in \Omega, \\ \mathrm{Id}_{jk} & \text{if } x \in G \setminus \overline{\Omega}, \end{cases}$$

$$\text{and} \quad \mu_{\text{eff}}(x) := \begin{cases} \int_Y 1 + k^2 w \chi_D \, dy & \text{if } x \in \Omega, \\ 1 & \text{if } x \in G \setminus \overline{\Omega}, \end{cases}$$

where w_j *and* w *are solutions to the following cell problems.* $w_j \in H^1_{\sharp,0}(Y^*)$, $j = 1, 2$, *solves*

$$\int_{Y^*} \varepsilon_e^{-1}(\mathbf{e}_j + \nabla_y w_j) \cdot \nabla_y \psi_1^* \, dy = 0 \quad \forall \psi_1 \in H^1_{\sharp,0}(Y^*) \tag{3.4}$$

and $w \in H^1_0(D)_\sharp$ *solves*

$$\int_D \varepsilon_i^{-1} \nabla_y w \cdot \nabla_y \psi_2^* - k^2 w \psi_2^* \, dy = \int_D \psi_2^* \, dy \quad \forall \psi_2 \in H^1_0(D)_\sharp. \tag{3.5}$$

The presentation is oriented at the results for diffusion problems in [2], which can be seen most prominently in the form of the effective permeability μ_{eff}. We prove that it is perfectly equivalent to the representation chosen in [11]; see Proposition 3.5.

The foregoing theorem means that in the limit $\delta \to 0$, the scatterer Ω can be described as a homogeneous material with the (effective) parameters a_{eff} (inverse permittivity) and μ_{eff}. Whereas a_{eff} is a positive definite matrix (see Proposition 3.5), the effective permeability μ_{eff} exhibits some astonishing properties: First of all, its occurrence itself is surprising as the scatterer is nonmagnetic. This is the already discussed effect of artificial magnetism. Second, the permeability is frequency dependent and its real part can have positive and negative signs. In the frequency region with $\mathrm{Re}(\mu_{\text{eff}}) < 0$ waves cannot propagate leading to photonic band gaps; see [11]. This effect is also studied numerically in detail in section 7.

We end with two observations on the two-scale equation, which are useful for the analysis later on. We introduce the "two-scale energy norm" on $\mathcal{H} := H^1(G) \times L^2(\Omega; H^1_{\sharp,0}(Y^*)) \times L^2(\Omega; H^1_0(D)_\sharp)$ as

$$\|(v, v_1, v_2)\|_e^2 := \|\nabla v + \nabla_y v_1\|^2_{G\times Y^*} + \|\nabla_y v_2\|^2_{\Omega\times D} + k^2\|v + \chi_D v_2\|^2_{G\times Y}. \tag{3.6}$$

In contrast to other homogenization settings, ∇v and $\nabla_y v_1$ as well as v and $\chi_D v_2$ are no longer orthogonal. Still, the two-scale energy norm is equivalent to the natural norm of $\mathcal{H}$, which is the statement of the next lemma.

LEMMA 3.3. *The two-scale energy norm is equivalent to the natural norm of* $\mathcal{H}$

$$\|(v, v_1, v_2)\|^2_{\mathcal{H}} := \|v\|^2_{H^1(G)} + \|v_1\|^2_{L^2(\Omega;H^1(Y^*))} + \|v_2\|^2_{L^2(\Omega;H^1(D))}.$$

Furthermore, the two-scale energy norm is equivalent to the k-dependent norm

$$\|(v, v_1, v_2)\|^2_{k,\mathcal{H}} := \|v\|^2_{1,k,G} + \|v_1\|^2_{L^2(\Omega;H^1(Y^*))} + \|v_2\|^2_{L^2(\Omega;1,k,D)},$$

where the equivalence constants do not depend on k and we have abbreviated

$$\|v_2\|^2_{L^2(\Omega;1,k,D)} := \|\nabla_y v_2\|^2_{L^2(\Omega;L^2(D))} + k^2\|v_2\|^2_{L^2(\Omega;L^2(D))}.$$

Proof. The essential ingredient is a sharpened Cauchy–Schwarz inequality for the nonorthogonal terms

$$\begin{aligned}\left|\int_G \int_{Y^*} \nabla v \cdot \nabla_y v_1 \, dy dx\right| &\le \|\nabla v\|_{L^2(G\times Y^*)} \|\nabla_y v_1\|_{L^2(G\times Y^*)} \\ &= |Y^*|^{1/2} \|\nabla v\|_{L^2(G)} \|\nabla_y v_1\|_{L^2(\Omega\times Y^*)}\end{aligned}$$

and $$\left|\int_G \int_Y v \chi_D v_2 \, dy dx\right| \le \|v\|_{L^2(G\times D)} \|v_2\|_{L^2(G\times D)} = |D|^{1/2}\|v\|_{L^2(G)}\|v_2\|_{L^2(\Omega;L^2(D))},$$

where $|Y^*|, |D| < 1$. ∎

LEMMA 3.4. *There exist constants $C_B > 0$ and $C_{\min} := \min\{1, \varepsilon_e^{-1}, \mathrm{Re}(\varepsilon_i^{-1})\} > 0$ depending only on the parameters and the geometry, such that $\mathcal{B}$ is continuous with constant C_B and fulfills a Gårding inequality with constant $C_{\min}$, i.e.,*

$$|\mathcal{B}(\mathbf{v}, \boldsymbol{\psi})| \le C_B \|\mathbf{v}\|_e \|\boldsymbol{\psi}\|_e \quad \textit{and} \quad \mathrm{Re}\,\mathcal{B}(\mathbf{v}, \mathbf{v}) + 2k^2\|v + \chi_D v_2\|^2_{G\times Y} \ge C_{\min}\|\mathbf{v}\|_e^2$$

for all $\mathbf{v} := (v, v_1, v_2), \boldsymbol{\psi} := (\psi, \psi_1, \psi_2) \in \mathcal{H}$.

Proof. The Gårding inequality is obvious from the definition of $\mathcal{B}$ in Theorem 3.1. The continuity of $\mathcal{B}$ follows from the multiplicative trace inequality as in [41]. ∎

3.2. Stability and regularity. In this section, we derive stability and regularity results for the two-scale equation and its homogenized formulation. To achieve that goal, we analyze the cell problems and the macroscopic equation separately. Although the homogenized macroscopic equation is of Helmholtz-type, the unusual effective parameters introduce new aspects and challenges in the stability analysis.

PROPOSITION 3.5. *The effective parameters in Ω have the following properties:*

1. a_{eff} *is a real-valued, symmetric, uniformly elliptic matrix.*
2. μ_{eff} *is a complex scalar with the upper bound on the absolute value*

$$|\mu_{\text{eff}}| \leq C_\mu \qquad \text{with } C_\mu = C(\varepsilon_i, D, Y, k_0). \tag{3.7}$$

3. μ_{eff} *can be equivalently written as*

$$\mu_{\text{eff}} = 1 + \sum_{n\in\mathbb{N}} \frac{k^2\varepsilon_i}{\lambda_n - k^2\varepsilon_i}\left(\int_D \phi_n\,dx\right)^2,$$

where (λ_n, ϕ_n) are the eigenvalues and eigenfunctions of the Laplace operator on D with Dirichlet boundary conditions.

4. *It holds that*

$$\operatorname{Im}(\mu_{\text{eff}}) \geq C(\varepsilon_i, D, Y)/k^2 > 0. \tag{3.8}$$

The proof is postponed to subsection 6.1. The upper and lower bound on μ_{eff} can only be obtained for $\operatorname{Im}(\varepsilon_i) > 0$. If we have an ideal lossless material (i.e., $\operatorname{Im}(\varepsilon_i) = 0$), μ_{eff} is unbounded; see [11]. As discussed above, the foregoing proposition shows that our μ_{eff} agrees with the one presented in [11]. However, we stress two advantages of our choice: First, it still holds for complex, but nonconstant parameters ε_i. Second, it only involves the solution of one cell problem rather than determining all eigenvalues and eigenfunctions of the Dirichlet Laplacian, which is very useful for the numerical implementation. The lower bound on $\operatorname{Im}(\mu_{\text{eff}})$ might be improved using sophisticated methods for estimating eigenvalues and averages of eigenfunctions of the Dirichlet Laplacian. We emphasize that our numerical experiment from section 7 does not show this severe k-dependence of the lower bound.

For the properties of the effective parameters, the cell problems have already been implicitly analyzed. Hence, results on the two-scale corrections u_1 and u_2 follow immediately.

PROPOSITION 3.6. *There are $C_{\text{stab},1}, C_{\text{stab},2} > 0$ depending only on ε_i^{-1}, ε_e^{-1}, D, Y^*, and k_0, such that the correctors u_1 and u_2 satisfy*

$$\|u_1\|_{L^2(\Omega;H^1(Y^*))} \leq C_{\text{stab},1}\|\nabla u\|_G \quad \text{and} \quad \|u_2\|_{L^2(\Omega;1,k,D)} \leq C_{\text{stab},2}\|u\|_{1,k,G}$$

with the notation $\|\cdot\|_{L^2(\Omega;1,k,D)}$ explained in Lemma 3.3.

All elements of the two-scale solution triple admit higher regularity depending on the geometry.

PROPOSITION 3.7. *Let $g \in H^{1/2}(\partial G)$. There are regularity coefficients $s(\Omega, G)$, $s(Y^*)$, and $s(D)$ with $s(\cdot) \in (\frac{1}{2}, 1]$ such that*

1. *for all $0 < s < s(D)$, $u_2 \in L^2(\Omega; H^{1+s}(D))$ with $\|u_2\|_{L^2(\Omega;H^{1+s}(D))} \leq C_{\text{reg},2}\, k\|u\|_{1,k,\Omega}$;*
2. *for all $0 < s < s(Y^*)$, $u_1 \in L^2(\Omega; H^{1+s}(Y^*))$ with $\|u_1\|_{L^2(\Omega;H^{1+s}(Y^*))} \leq C_{\text{reg},1}\, \|\nabla u\|_\Omega$;*

3. *for all* $0 < s < s(\Omega, G)$, $u \in H^{1+s}_{pw}(G)$ *(see* (2.1)*) with*

$$\|u\|_{H^{1+s}_{pw}(G)} \leq C(k\|u\|_{1,k,G} + \|f\|_G + \|g\|_{H^{1/2}(\partial G)}). \tag{3.9}$$

Proof. The assertion follows from classical regularity theory for elliptic and interface problems; see [50]. We also refer to regularity results for the standard Helmholtz equation as in [41], for instance. ∎

With a C^2 boundary of D (and then also Y^*), we obtain $s(D) = s(Y^*) = 1$. For the numerical treatment, D is approximated by a polygonally bounded Lipschitz domain. As also $\partial\Omega$ is of class C^2 and G is convex, we have $s(\Omega, G) = 1$. The interface $\partial\Omega$ is also approximated by a piecewise polygonal interface in practical numerical schemes. In general, the maximal regularity of the problems posed on a polygonal Lipschitz domain depends on the domain's maximal interior angle; see [50]. We give the regularity results in their general form as polygonal (nonconvex) domains have to be considered in the process of boundary approximation in sections 4 and 5.

Looking at estimate (3.9), we note that we need an estimate for $\|u\|_{1,k,G}$ in terms of the data. From Fredholm theory we have a stability estimate of the form $\|u\|_{1,k,G} \leq C(k)\|g\|_{\partial G}$, but the dependence of the constant on the wavenumber k is unknown. We therefore make the following assumption of polynomial stability.

Assumption 3.8. Assume that there is $q \in \mathbb{N}_0$ and $C_{\text{stab},0} > 0$ such that the solution u to (3.2) with additional right-hand side $f \in L^2(G)$ fulfills

$$\|u\|_{1,k,G} \leq C_{\text{stab},0}\, k^q(\|f\|_G + \|g\|_{H^{1/2}(\partial G)}).$$

Polynomial stability is not trivial: There are so called trapping domains leading to exponential growth of the stability estimate in k; see [8]. In our setting, we can prove the assumption with $q = 3$ under some (mild) additional assumptions. More explicitly speaking, we have the following theorem, which is proved in subsection 6.2.

THEOREM 3.9 (stability). *Assume that there is* $\gamma > 0$ *such that*

$$x \cdot n_G \geq \gamma \text{ on } \partial G, \qquad\qquad x \cdot n_\Omega \geq 0 \text{ on } \partial\Omega, \tag{3.10}$$

where n *denotes the outer normal of the domain specified in the subscript. Furthermore assume that* $a_{\text{eff}}|_{G\setminus\overline{\Omega}} - a_{\text{eff}}|_\Omega$ *is negative semidefinite. Let* u *be the solution to* (3.2) *with additional volume term* $\int_G f\phi^*\,dx$ *on the right-hand side for* $f \in L^2(G)$. *Then there is* $C_{\text{stab},0}$ *only depending on the geometry, the parameters, and* k_0*, such that* u *satisfies the stability estimate*

$$\|u\|_{1,k,G} \leq C_{\text{stab},0}\left(k^3\|f\|_{G\setminus\overline{\Omega}} + k^2\|f\|_\Omega + k^{3/2}\|g\|_{\partial G} + k^{-1}\|g\|_{H^{1/2}(\partial G)}\right).$$

The geometrical assumption (3.10) is the common assumption for scattering problems; see [24, 33, 43]. It can, for example, be fulfilled if Ω is convex (and without loss of generality (w.l.o.g.) $0 \in \Omega$) and G is chosen appropriately. The assumption on a_{eff} in fact is an assumption on ε_e and can be fulfilled for appropriate choices of material inside and outside the scatterer. Analytically, this assumption can be traced back to the assumption that "$Da \cdot x$ is negative semidefinite" for Lipschitz continuous a in Proposition 6.1. In order to obtain that proposition, a weaker condition on the Lipschitz constant of a would be sufficient, but then the constant in the stability estimate would depend on the Lipschitz constant of a, which blows up in the approximation of a_{eff}. We emphasize that a similar condition on the derivative of the diffusion coefficient and/or its Lipschitz constant has also been imposed in the scalar case in [14].

In the literature, most stability results for Helmholtz problems have been obtained in the case of constant coefficients; see, e.g., [5, 24, 33, 41, 42, 43]. Only recently scalar valued, Lipschitz continuous real-valued heterogeneous coefficients have been studied in [14]. All these works have obtained the stability estimate with $q = 0$ under the same geometry assumption (3.10) as here. Our setting exhibits three new challenges for the stability analysis: a discontinuous, namely, piecewise constant, diffusion coefficient, a partly complex parameter μ, and the fact that the diffusion coefficient a is matrix valued. The second aspect introduces the worse dependence on k in the stability estimate, as explained after Proposition 6.1. There, we also discuss how the lower bound on the imaginary part of μ influences the stability estimate.

Under the assumption of polynomial stability, the (final) stability and regularity estimates for the two-scale equation are deduced. A bound on the inf-sup-constant of the corresponding sesquilinear form is obtained similarly to [33, 41, 49].

Proposition 3.10. *If Assumption* 3.8 *is satisfied, the following hold:*

1. *The two-scale solution satisfies*

$$\|(u, u_1, u_2)\|_e \leq C_{\mathrm{stab},e}\, k^q(\|f\|_G + \|g\|_{H^{1/2}(\partial G)})$$

for $C_{\mathrm{stab},e} := C_{\mathrm{stab},0}(1 + C_{\mathrm{stab},1} + C_{\mathrm{stab},2})$.

2. *The regularity estimate for* u *is*

$$\|u\|_{H^{1+s}_{pw}(G)} \leq C_{\mathrm{reg},0}\, k^{q+1}(\|f\|_G + \|g\|_{H^{1/2}(\partial G)}).$$

3. *The inf-sup-constants of* B_{eff} *and* $\mathcal{B}$ *can be bounded below as follows:*

$$\inf_{v\in H^1(G)} \sup_{\psi\in H^1(G)} \frac{\operatorname{Re} B_{\mathrm{eff}}(v,\psi)}{\|v\|_{H^1(G)}\|\psi\|_{H^1(G)}} \geq C_{\mathrm{inf,eff}} k^{-(q+1)}, \tag{3.11}$$

$$\inf_{\mathbf{v}\in\mathcal{H}} \sup_{\boldsymbol{\psi}\in\mathcal{H}} \frac{\operatorname{Re}\mathcal{B}(\mathbf{v},\boldsymbol{\psi})}{\|\mathbf{v}\|_e\|\boldsymbol{\psi}\|_e} \geq C_{\mathrm{inf},e} k^{-(q+1)} \tag{3.12}$$

with $C_{\mathrm{inf,eff}} := \min\{\alpha, C_\mu\}(k_0^{-(q+1)} + C_{\mathrm{stab},0})^{-1}$, *where* α *denotes the ellipticity constant of* a_{eff}, *and* $C_{\mathrm{inf},e} := \min\{C_{\min}, 1\}(k_0^{-(q+1)} + C_{\mathrm{stab},e})^{-1}$.

4. The HMM. As explained in the introduction, a direct discretization of the heterogeneous problem (2.3) is infeasible due to the necessary small grid mesh width resolving all inclusions. The idea of the HMM is to imitate the homogenization process and to thereby provide a method based on grids independent of the finescale parameter δ. In this paper, we introduce the HMM as a direct discretization of the two-scale equation (3.1); see [46] for the original idea for elliptic diffusion problems. This point of view is vital for the numerical analysis in section 5 since ideas and procedures developed for "normal" Helmholtz problems can be easily transferred. However, we will also shortly explain below how this direct discretization can be decoupled into macroscopic and microscopic computations in the fashion of the HMM as originally presented in [20, 21].

In this and the next section, we assume that D and Ω are polygonally bounded (in contrast to the C^2 boundaries in the analytic sections). The reason is that the C^2 boundaries can be approximated by a series of more and better fitting polygonal boundaries. This procedure of boundary approximation results in nonconforming methods, i.e., the discrete function spaces are no subspaces of the analytic ones. We avoid this difficulty in our numerical analysis by assuming polygonally bounded domains by now. The new assumption reduces the possible higher regularity of solutions as discussed in subsection 3.2. However, we can always obtain the maximal regularity in the limit of polygonal approximation of C^2 boundaries, which we have in mind as an application case.

Denote by $\mathcal{T}_H = \{T_j | j \in J\}$ and $\mathcal{T}_h = \{S_k | k \in I\}$ conforming and shape regular triangulations of G and Y, respectively. Additionally, we assume that $\mathcal{T}_H$ resolves the partition into Ω and $G \setminus \overline{\Omega}$ and that $\mathcal{T}_h$ resolves the partition of Y into D and Y^* and is periodic in the sense that it can be wrapped to a regular triangulation of the torus (without hanging nodes). By $\mathcal{T}_h(Y^*)$ and $\mathcal{T}_h(D)$, we denote the parts of the triangulation $\mathcal{T}_h$ belonging to Y^* and D, respectively. We define the local mesh sizes $H_j := \operatorname{diam}(T_j)$ and $h_k := \operatorname{diam}(S_k)$ and the global mesh sizes $H := \max_{j \in J} H_j$ and $h := \max_{k \in I} h_k$. Finally, the discrete function spaces $V_H^1 \subset H^1(G)$, $\widetilde{V}_h^1(Y^*) \subset H^1_{\sharp,0}(Y^*)$, and $V_h^1(D) \subset H^1_0(D)_\sharp$ are defined as

$$
\begin{aligned}
V_H^1 &:= \left\{ v_H \in H^1(G) | v_H|_T \in \mathbb{P}^1 \quad \forall T \in \mathcal{T}_H \right\}, \\
\widetilde{V}_h^1(Y^*) &:= \left\{ v_h \in H^1_{\sharp,0}(Y^*) | v_h|_S \in \mathbb{P}^1 \quad \forall S \in \mathcal{T}_h(Y^*) \right\}, \\
V_h^1(D) &:= \left\{ v_h \in H^1_0(D)_\sharp | v_h|_S \in \mathbb{P}^1 \quad \forall S \in \mathcal{T}_h(D) \right\},
\end{aligned}
$$

where $\mathbb{P}^1$ are the linear polynomials. In other words, we use standard linear finite element spaces (with obvious adaptations to the boundary conditions) to discretize the function spaces $H^1(G)$, $H^1_{\sharp,0}(Y^*)$, and $H^1_0(G)$.

Definition 4.1. *The discrete two-scale solution*

$$
(u_H, u_{h,1}, u_{h,2}) \in V_H^1 \times L^2\left(\Omega; \widetilde{V}_h^1(Y^*)\right) \times L^2\left(\Omega; V_h^1(D)\right)
$$

is defined as the solution of

$$
\begin{aligned}
\mathcal{B}((u_H, u_{h,1}, u_{h,2}), (\psi_H, \psi_{h,1}, \psi_{h,2})) &= \int_{\partial G} g\, \psi_H^* \, d\sigma \\
&\forall (\psi_H, \psi_{h,1}, \psi_{h,2}) \in V_H^1 \times L^2\left(\Omega; \widetilde{V}_h^1(Y^*)\right) \times L^2\left(\Omega; V_h^1(D)\right)
\end{aligned}
\tag{4.1}
$$

with the two-scale sesquilinear form $\mathcal{B}$ defined in Theorem 3.1.

In order to evaluate the integrals over G in $\mathcal{B}$, one introduces quadrature rules, which are exact for the given ansatz and test spaces. In our case of piecewise linear functions, it suffices to choose the one-point rule $\{|T_j|, x_j\}$ with the barycenter x_j for the gradient part and a second order quadrature rule $Q_j^{(2)} := \{q_l, x_l\}_l$ with $l = 1, 2, 3$ on each triangle T_j for the identity part. As a consequence, the functions $u_{h,1}$ and $u_{h,2}$ will also be discretized with respect to the macroscopic variable x: In fact, one has $u_{h,1} \in S_H^0(\Omega; \widetilde{V}_h^1(Y^*))$ and $u_{h,2} \in S_H^1(\Omega; V_h^1(D))$. Here, the space of discontinuous, piecewise p-polynomial (w.r.t. x) discrete functions is defined as

$$S_H^p(\Omega; X_h) := \left\{v_h \in L^2(\Omega; X) \,|\, v_h(\cdot, y)|_{T_j} \in \mathbb{P}^p \;\forall j \in J, y \in Y; v_h(x, \cdot) \in X_h \;\forall x \in \Omega\right\}$$

for any conforming finite element space $X_h \subset X$. In other words, a discrete function in $S_H^p(\Omega; X_h)$ is a (discontinuous) piecewise p-polynomial with respect to the first variable x and belongs to the discrete space X_h in the second variable. We have $X_h = \widetilde{V}_h^1(Y^*)$ and $p = 0$ for $u_{h,1}$ and $X_h = V_h^1(D)$ and $p = 1$ for $u_{h,2}$. Note that $u_{h,2}$ is a piecewise x-linear discrete function, since $Q^{(2)}$ consists of 3 quadrature points on each triangle.

The functions $u_{h,1}$ and $u_{h,2}$ are the discrete counterparts of the analytical correctors u_1 and u_2. They are correctors to the macroscopic discrete function u_H and solve discretized cell problems. These cell problems, posed in the unit square Y, can be transferred back to δ-scaled and shifted unit squares $Y_j^\delta = x_j + \delta Y$, where x_j is a macroscopic quadrature point. This finally gives an equivalent formulation of (4.1) in the form of a (traditional) HMM. The formulation using a macroscopic sesquilinear form with local cell reconstructions is used in practical implementations. We emphasize that the presented HMM also works for locally periodic ε^{-1} depending on x and y. The HMM and its interpretation as a discretization of a fully coupled two-scale equation can even be applied to nonperiodic problems, as demonstrated in [31].

5. Quasi-optimality of the HMM. Based on the definition of the HMM in Definition 4.1, we analyze its quasi-optimality in Theorem 5.1. This quasi-optimality is a kind of Céa lemma for indefinite sesquilinear forms and directly leads to a priori estimates.

All estimates will be derived in the two-scale energy norm (3.6). Let us furthermore define the error terms $e_0 := u - u_H$, $e_1 := u_1 - u_{h,1}$, and $e_2 := u_2 - u_{h,2}$. We will only estimate these errors and leave the modeling error $u_\delta - (u_H + u_{h,2}(\cdot, \frac{\cdot}{\delta}) + \delta u_{h,1}(\cdot, \frac{\cdot}{\delta}))$, introduced by homogenization, apart. Unfortunately, there is no estimate in δ available in the literature for this modeling error. Recall the abbreviation $\mathcal{H} := H^1(G) \times L^2(\Omega; H^1_{\sharp,0}(Y^*)) \times L^2(\Omega; H^1_0(D)_\sharp)$. In a similar short form we write $\mathbf{V}_{H,h} := V_H^1 \times L^2(\Omega; \widetilde{V}_h^1(Y^*)) \times L^2(\Omega; V_h^1(D))$.

We recall that the finite element function space $\mathbf{V}_{H,h}$ has the following approximation property: There is C_{appr} such that for all $\frac{1}{2} < s \leq 1$ and given $(v, v_1, v_2) \in H^{1+s}_{pw}(G) \times L^2(\Omega; H^{1+s}(Y^*)) \times L^2(\Omega; H^{1+s}(D))$ it holds

$$\begin{aligned} (\|v - v_H\|_G + H\|\nabla(v - v_H)\|_G) &\leq C_{\text{appr}} H^{1+s} |v|_{H^{1+s}_{pw}(G)}, \\ (\|v_1 - v_{h,1}\|_{\Omega \times Y^*} + h\|\nabla_y(v_1 - v_{h,1})\|_{\Omega\times Y^*}) &\leq C_{\text{appr}} h^{1+s} |v_1|_{L^2(\Omega; H^{1+s}(Y^*))}, \\ (\|v_2 - v_{h,2}\|_{\Omega\times D} + h\|\nabla_y(v_2 - v_{h,2})\|_{\Omega\times D}) &\leq C_{\text{appr}} h^{1+s} |v_2|_{L^2(\Omega; H^{1+s}(D))} \end{aligned} \tag{5.1}$$

for all $\mathbf{v}_{H,h} := (v_H, v_{h,1}, v_{h,2}) \in \mathbf{V}_{H,h}$. The space $H^{1+s}_{pw}(G)$ is defined in (2.1). Note that the regularity coefficient s does not necessarily have to be the same in all three estimates.

In the h-version of the finite element method we consider in this paper, the meshes $\mathcal{T}_H$ and $\mathcal{T}_h$ are refined (thus decreasing H and h) in order to obtain a better approximation. Hence, we introduce constants $H_{\max} > 0$ and $h_{\max} > 0$ such that $H \leq H_{\max}$ and $h \leq h_{\max}$ for all considered grids.

THEOREM 5.1 (discrete inf-sup-stability and quasi-optimality). *Let Assumption 3.8 be satisfied and let $s(\Omega, G)$, $s(Y^*)$, and $s(D)$ be the (higher) regularity exponents from Proposition 3.7. Fix (s_0, s_1, s_2) with $0 < s_0 < s(\Omega, G)$, $0 < s_1 < s(Y^*)$,*

$0 < s_2 < s(D)$. *If the wavenumber k and the mesh widths H, h are coupled by*

$$
\begin{aligned}
&k^{q+2}H^{s_0} \le -\frac{k_0^{q+1}}{2H_{\max}^{1-s_0}} + \sqrt{\frac{k_0^{q+1}}{H_{\max}^{1-s_0}}\left(\frac{C_{\min}}{12C_B C_{\mathrm{appr}} C_{\mathrm{reg},0}} + \frac{k_0^{q+1}}{4H_{\max}^{1-s_0}}\right)},\\
&k^{q+1}h^{s_1} \le \frac{C_{\min}}{12C_B C_{\mathrm{appr}} C_{\mathrm{reg},1} C_{\mathrm{stab},e}},\\
&k^{q+2}h^{s_2} \le -\frac{k_0^{q+1}}{2h_{\max}^{1-s_2}} + \sqrt{\frac{k_0^{q+1}}{h_{\max}^{1-s_2}}\left(\frac{C_{\min}}{12C_B C_{\mathrm{appr}} C_{\mathrm{reg},2} C_{\mathrm{stab},e}} + \frac{k_0^{q+1}}{4h_{\max}^{1-s_2}}\right)},
\end{aligned}
\tag{5.2}
$$

then

$$
\inf_{\mathbf{v}_{H,h}\in \mathbf{V}_{H,h}} \sup_{\boldsymbol{\psi}_{H,h}\in \mathbf{V}_{H,h}} \frac{\operatorname{Re}\mathcal{B}(\mathbf{v}_{H,h},\boldsymbol{\psi}_{H,h})}{\|\mathbf{v}_{H,h}\|_e\,\|\boldsymbol{\psi}_{H,h}\|_e} \ge \frac{C_{\mathrm{HMM}}}{k^{q+1}}
\tag{5.3}
$$

with $C_{\mathrm{HMM}} := \frac{C_{\min}}{2}(k_0^{-(q+1)}(1+\frac{C_{\min}}{2C_B})+C_{\mathrm{stab},e})^{-1}$ *and the error between the two-scale solution and the HMM-approximation satisfies*

$$
\|(e_0,e_1,e_2)\|_e \le \frac{2C_B}{C_{\min}} \inf_{\mathbf{v}_H\in\mathbf{V}_{H,h}} \|\mathbf{u}-\mathbf{v}_H\|_e \le C\left((H^{s_0}+h^{s_2})k^{q+1}+k^q h^{s_1}\right)\|g\|_{H^{1/2}(\partial G)}.
\tag{5.4}
$$

The proof is postponed to subsection 6.3.

Corollary 5.2. *Under the maximal possible regularity $s_0 = s_1 = s_2 = 1$ as discussed in subsection* 3.2*, the energy error converges with rate $k^{q+1}(H+h)$ under the resolution assumption that $k^{q+2}(H+h)$ is sufficiently small.*

Dual problems can be used to estimate $\|(e_0,e_1,e_2)\|_{L^2}$ by

$$C(k^{q+1}(H^{s_0}+h^{s_2})+k^q h^{s_1})\|(e_0,e_1,e_2)\|_e$$

as in the the proof of Theorem 5.1. This is the classical Aubin–Nitsche argument to obtain higher convergence rates in the L^2-norm; for details see [25, 42] for classical Helmholtz problems.

As has already been remarked in [32, 46], the definition of the HMM as a direct discretization of the two-scale equation (see (4.1)), is the crucial starting point for all kinds of error estimates and, in particular, enables us to derive a posteriori error estimates. This can also be achieved for the setting considered here by adapting a posteriori error estimates for Helmholtz problems obtained e.g., in [19, 37] to the two-scale equation.

Under the regularity estimate from Assumption 3.8, the resolution condition (5.2) is optimal/unavoidable for standard finite element methods and the multiscale setting: As the second cell problem depends on k, it is natural that h enters the condition (5.2). We emphasize that h denotes the mesh width of the unit square mesh and is thus not coupled to δ in any way. Assuming now $q = 0$, as is the case for classical Helmholtz problems, we regain the usual condition "$k^2(H+h)$ sufficiently small"; cf., e.g., [24, 33, 36, 41, 42]; see also the early abstract discussion in [52]. This is also the resolution condition we experience in our numerical experiments in section 7. Our explicit stability estimate in Theorem 3.9 yields $q = 3$ and thus, the resolution condition "$k^5(H+h)$ small". This is a kind of "worst case" resolution condition: It is certainly sufficient for the quasi-optimality and a priori error result presented above, but can well (as the numerical example indicates) be suboptimal. We emphasize that this gap between the optimal and worst case resolution condition is no defect of the numerical method, but can be closed if better stability results in the spirit of Theorem 3.9 are proved, which is outside the scope of our work.

As also supported by our numerical experiment, the HMM is much more efficient than a direct discretization of the heterogeneous Helmholtz problem (2.3). In order to get an accurate solution, one needs a grid with mesh size h_{ref} satisfying $h_{\text{ref}} < \delta \ll 1$ from the multiscale point of view. On top of that, at least $k^2 h_{\text{ref}} < C$ has to be satisfied to rule out preasymptotic effects. Note that the heterogeneous problem does not fulfill the assumptions for any available stability estimate, so that the resolution condition may even be worse.

Although the so-called pollution effect is not avoidable for the classical Helmholtz equation in dimension $d \geq 2$ as shown in [4], much work in its reduction has been invested: Examples of the proposed methods are the *hp*-version of the finite element method [24, 42], (hybridizable) discontinuous Galerkin methods [16, 30], or plane wave Trefftz methods [35, 34, 48], just to name a few. Recently, it has been shown that the resolution condition can be relaxed to the natural assumption kh sufficiently small by applying a localized orthogonal decomposition (LOD) to the Hemholtz equation; see [14, 27, 49]. The function space is decomposed into a coarse space, where the solution is sought, and a remainder space. The coarse space is spanned by pre-computable basis functions with local support, which include some information from the remainder space by the solution of localized correction problems. The definition of the HMM as a direct discretization of the two-scale equation makes it possible to apply an additional LOD; see [47].

6. Main proofs. In this section the essential proofs of the properties of the effective parameters occurring in homogenization, the stability of the effective equation, and the quasi-optimality of the HMM will be given.

6.1. Proof of the properties of the effective parameters. In this section we show the upper and lower bounds for the effective permeability μ_{eff}. We also show the equivalence of the two formulations of μ_{eff} obtained from Allaire [2] and Bouchitté, Bourel, and Felbacq [10], respectively.

Proof of Proposition 3.5. The characterization of a_{eff} is well known and follows from the ellipticity of the corresponding cell problem (3.4); see [2] for similar cell problems.

Cell problem (3.5) is (uniformly) coercive because of $\operatorname{Im}(\varepsilon_i^{-1}) < 0$. The Lax–Milgram–Babuška theorem [3] now implies the unique solvability of the cell problem for w with the stability estimate

$$\|w\|_{1,k,D} \leq C(\varepsilon_i, k_0, D)/k.$$

Combination with the representation of μ_{eff} directly yields (3.7).

It is well known that the eigenfunctions of the Laplace operator on D with Dirichlet boundary conditions form an orthonormal basis of $L^2(D)$. The eigenvalues λ_n are sorted as a positive, increasing sequence of real numbers. We have the representation $1 = \sum_n (\int_D \phi_n)\phi_n$. Writing $w = \sum_n \alpha_n \phi_n$ and inserting this into (3.5), gives after a comparison of coefficients

$$w = \sum_n \left(\frac{\varepsilon_i}{\lambda_n - k^2 \varepsilon_i} \int_D \phi_n \right) \phi_n \quad \text{and, hence,} \quad \mu_{\text{eff}} = 1 + \sum_n \frac{k^2 \varepsilon_i}{\lambda_n - k^2 \varepsilon_i} \left(\int_D \phi_n \right)^2;$$

see [11]. A similar computation for the full three-dimensional case is given in [38, Appendix A]. Now we can deduce because of the positivity of $\operatorname{Im}(\varepsilon_i)$ and of the eigenvalues that

$$\operatorname{Im}(\mu_{\text{eff}}) = \sum_n \frac{k^2\lambda_n \operatorname{Im}(\varepsilon_i)}{|\lambda_n - k^2\varepsilon_i|^2}\left(\int_D \phi_n\right)^2 \geq \frac{k^2\lambda_0 \operatorname{Im}(\varepsilon_i)}{|\lambda_0 - k^2\varepsilon_i|^2}\left(\int_D \phi_0\right)^2.$$

The first eigenfunction of the Dirichlet Laplacian is zero free, thus $(\int_D \phi_0)^2 > 0$. As we consider the high-frequency case, we can w.l.o.g. assume $\lambda_0 \leq k^2|\varepsilon_i|$ and then obtain $|\lambda_0 - k^2\varepsilon_i|^2 \leq 2k^4|\varepsilon_i|^2$. This finally gives

$$\operatorname{Im}(\mu_{\text{eff}}) \geq \frac{k^2\lambda_0 \operatorname{Im}(\varepsilon_i)}{2k^4|\varepsilon_i|^2}\left(\int_D \phi_0\right)^2 \geq \frac{C(\varepsilon_i, D)}{k^2} > 0. \qquad \square$$

6.2. Polynomial stability of the Helmholtz equation with discontinuous coefficients. In this section, we give a detailed proof of Theorem 3.9. We consider a Lipschitz continuous, matrix-valued diffusion coefficient a with the partly complex-valued μ first. Then the discontinuity in a_{eff} is treated by a smoothing/approximation procedure. A direct application of the Rellich–Morawetz identities (see, e.g., [43, section 2] and the references therein) is not possible due to jumps in the gradient of the solution over the interface. Throughout this subsection, we use the notation $a \lesssim b$ for $a \leq Cb$ with a constant C independent of k, η, and c_0.

PROPOSITION 6.1. *Let Ω and G satisfy* (3.10). *Let u be the unique solution to*

$$B(u, \psi) = (f, \psi)_G + (g, \psi)_{\partial G}$$

for $f \in L^2(G)$ and $g \in L^2(\partial G)$, where B is the sesquilinear form of (3.3) *with a_{eff} replaced by a and μ_{eff} replaced by μ fulfilling the assumptions*

- *$a \in W^{1,\infty}(G, \mathbb{R}^{2\times 2})$ is symmetric, bounded, and uniformly elliptic;*
- *the matrix $Da \cdot x$ with $(Da \cdot x)_{ij} := \sum_k x_k\, \partial_k a_{ij}$ is negative semidefinite;*
- *$\mu \in L^\infty(G; \mathbb{C})$ is piecewise constant, namely, $\mu = \mu_2 \in \mathbb{R}_+$ in $G \setminus \overline{\Omega}$ and $\mu = \mu_1 \in \mathbb{C}$ in Ω with $\operatorname{Im}(\mu_1) > c_0 > 0$.*

Then the following stability estimate holds,

$$\begin{aligned}\|u\|_{1,k,G} \lesssim\, & k^{1/2}\left(c_0^{-1/2} + 1\right)\|g\|_{\partial G} + \|f\|_G + \left(c_0^{-1/2} + c_0^{-1}\right)\|f\|_\Omega \\ & + \frac{1}{k}\left(1 + c_0^{-1/2} + c_0^{-1}\right)\|f\|_G + \frac{k}{c_0}\|f\|_{G\setminus\overline{\Omega}},\end{aligned}$$

where the constants depend on the geometry, the upper bounds on μ and a, the ellipticity constant of a, and on k_0; but not on the Lipschitz constant of a or any other constant involving the derivative of a.

Proof. First step: With $\psi = u$ and considering the imaginary part, we obtain with Hölder's and Young's inequalities

$$k^2 c_0\|u\|_\Omega^2 + k\|u\|_{\partial G}^2 \lesssim \left(\frac{1}{k}\|g\|_{\partial G}^2 + \frac{1}{k^2 c_0}\|f\|_\Omega^2 + \|f\|_{G\setminus\overline{\Omega}}\|u\|_{G\setminus\overline{\Omega}}\right). \tag{6.1}$$

Second step: With $\psi = u$ and considering the real part, we obtain due to the boundedness of μ and the uniform ellipticity of a

$$\|\nabla u\|_G^2 \lesssim \left(k^2\|u\|_G^2 + \frac{1}{2k^2}\|f\|_G^2 + \frac{k^2}{2}\|u\|_G^2 + \|g\|_{\partial G}\|u\|_{\partial G}\right).$$

Inserting (6.1) yields

$$\|\nabla u\|_G^2 \lesssim \left(k^2\|u\|^2_{G\setminus\overline{\Omega}} + \frac{1}{k^2}\left(1+\frac{1}{c_0^2}\right)\|f\|_G + \frac{1}{k^2c_0}\|f\|^2_\Omega + \frac{1}{k}\left(\frac{1}{c_0}+1\right)\|g\|^2_{\partial G}\right). \tag{6.2}$$

Third step: It remains to estimate $\|u\|^2_{G\setminus\overline{\Omega}}$. For this, we insert $\psi = x\cdot\nabla u$ and consider the real part. Note that $x\cdot\nabla u$ is an admissible test function because we have $u\in H^2(G)$ due to the convexity of G and the smoothness of a; see [28]. We moreover use the identity $\partial_j(|w|^2) = 2\operatorname{Re}(w\partial_j w^*)$. For the first term of the sesquilinear form we obtain

$$\begin{aligned}
&\operatorname{Re}\int_G a\nabla u\cdot\nabla(x\cdot\nabla u^*)\,dx\\
&\quad= \operatorname{Re}\int_G a\nabla u\cdot\nabla u^* + a\nabla u\cdot\left(D^2u^*\right)x\,dx\\
&\quad= \int_G a\nabla u\cdot\nabla u^* + \frac{1}{2}\nabla(a\nabla u\cdot\nabla u^*)\cdot x - \frac{1}{2}(Da\cdot x)\nabla u\cdot\nabla u^*\,dx\\
&\quad= -\frac{1}{2}\int_G(Da\cdot x)\nabla u\cdot\nabla u^*\,dx + \frac{1}{2}\int_{\partial G} a\nabla u\cdot\nabla u^* x\cdot n\,d\sigma,
\end{aligned}$$

where in the last equality we integrated by parts. As $Da\cdot x$ is negative semidefinite by the assumption, the first term is nonnegative.

For the second part of the sesquilinear form we obtain

$$\begin{aligned}
&\operatorname{Re}\int_G k^2\mu u x\cdot\nabla u^*\,dx\\
&\quad= \operatorname{Re}\int_\Omega k^2\mu_1 u x\cdot\nabla u^*\,dx + \frac{\mu_2}{2}\int_{G\setminus\overline{\Omega}} k^2 x\cdot\nabla|u|^2\,dx\\
&\quad= \operatorname{Re}\int_\Omega k^2\mu_1 u x\cdot\nabla u^*\,dx + \frac{\mu_2}{2}\int_{\partial(G\setminus\overline{\Omega})} k^2|u|^2 x\cdot n\,d\sigma - \int_{G\setminus\overline{\Omega}} k^2\mu_2|u|^2\,dx.
\end{aligned}$$

So for the test function $\psi = x\cdot\nabla u$ and the real part we deduce by combining the foregoing calculations

$$\begin{aligned}
&\frac{1}{2}\int_{\partial G} a\nabla u\cdot\nabla u^* x\cdot n\,d\sigma + \int_{G\setminus\overline{\Omega}} k^2\mu_2|u|^2\,dx\\
&\quad\le \frac{1}{2}\int_{\partial(G\setminus\overline{\Omega})} k^2\mu_2|u|^2 x\cdot n\,d\sigma + \operatorname{Re}\left(\int_\Omega k^2\mu_1 u x\cdot\nabla u^*\,dx + \int_{\partial G} iku x\cdot\nabla u^*\,d\sigma\right)\\
&\qquad+ \operatorname{Re}\left(\int_G f x\cdot\nabla u^*\,dx + \int_{\partial G} g x\cdot\nabla u^*\,d\sigma\right).
\end{aligned}$$

The assumption (3.10) on G and Ω implies that the first term on the right-hand side can be bounded above by $k^2\|u\|^2_{\partial G}$. This yields after application of Hölder's and Young's inequalities

$$k^2\|u\|^2_{G\setminus\overline{\Omega}} \lesssim \left(k^2\|u\|_\Omega\|\nabla u\|_\Omega + k^2\|u\|^2_{\partial G} + \|g\|^2_{\partial G} + \|f\|_G\|\nabla u\|_G\right).$$

Inserting the estimates (6.1) and (6.2) into the estimate for $k^2\|u\|^2_{G\setminus\overline{\Omega}}$ gives

$$k^2\|u\|^2_{G\setminus\overline{\Omega}} \lesssim \Bigg(\|g\|^2_{\partial G} + \frac{1}{kc_0}\|f\|^2_{\Omega} + \eta_1 k^2\|u\|^2_{G\setminus\overline{\Omega}} + \frac{1}{\eta_1}\|f\|^2_{G\setminus\overline{\Omega}} + \frac{1}{\eta_2}\|f\|^2_G + \eta_2 k^2\|u\|^2_{G\setminus\overline{\Omega}} + \frac{\eta_2}{k^2}\left(1+c_0^{-2}\right)\|f\|^2_G + \frac{\eta_2}{k^2c_0}\|f\|^2_\Omega + \frac{\eta_2}{k}\left(1+c_0^{-1}\right)\|g\|^2_{\partial G} + \frac{k^4}{\delta_2}\|u\|^2_\Omega\Bigg).$$

Choose η_1, η_2 independent of k such that $k^2\|u\|_{G\setminus\overline{\Omega}}$ can be hidden on the left-hand side and insert once more (6.1) for the last term on the right-hand side to obtain

$$\begin{aligned}k^2\|u\|^2_{G\setminus\overline{\Omega}} \lesssim \Bigg(&\|g\|^2_{\partial G} + \|f\|^2_G + \left(\frac{1}{kc_0} + \frac{1}{k^2c_0}\right)\|f\|^2_\Omega + \left(\frac{1}{k^2} + \frac{1}{k^2c_0^2}\right)\|f\|^2_G \\ &+ \left(\frac{1}{k} + \frac{1}{kc_0}\right)\|g\|^2_{\partial G} + \frac{k}{c_0}\|g\|^2_{\partial G} + \frac{1}{c_0^2}\|f\|^2_\Omega \\ &+ \eta_3 k^2\|u\|^2_{G\setminus\overline{\Omega}} + \frac{k^2}{\eta_3 c_0^2}\|f\|^2_{G\setminus\overline{\Omega}}\Bigg).\end{aligned}$$

Choosing finally η_3 appropriately gives the desired estimate for $k^2\|u\|^2_{G\setminus\overline{\Omega}}$ and combination with (6.1) and (6.2) finishes the proof. □

If c_0 is independent from k, we obtain

$$\|u\|_{1,k,G} \lesssim \left(\|f\|_\Omega + k\|f\|_{G\setminus\overline{\Omega}} + k^{1/2}\|g\|_{\partial G}\right).$$

On the other hand, if $c_0 > k^{-2}$ as in the case of μ_{eff} (see Proposition 3.5), we obtain

$$\|u\|_{1,k,G} \lesssim \left(k^2\|f\|_\Omega + k^3\|f\|_{G\setminus\overline{\Omega}} + k^{3/2}\|g\|_{\partial G}\right).$$

The dependence of c_0 on k contributes by a factor k for g and a factor k^2 for f. However, even without this critical dependence of c_0 on k, the stability estimate is worse than the classical versions by about a factor k for f and $k^{1/2}$ for g. Looking into the proof, one can see that this is due to the difficult term $\int_\Omega k^2\mu u x\cdot\nabla u$.

The presented proof can also be transferred (with minor adaptations) to the case where μ is a real constant and then yields the known stability of k^0. So this also contributes to the analysis of [14] by covering the case of matrix valued a.

Proof of Theorem 3.9. Because of the density of smooth functions in L^p for $p \in [1,\infty)$, for every $\eta > 0$ there exists $a_\eta \in C^\infty(\overline{G})$ such that $\|a_\eta - a\|_{L^p} \leq \eta$. Furthermore, a_η can be chosen symmetric and uniformly elliptic with constants independent of η. Because of the additional assumption on a_{eff} and the geometric setting, the assumption $Da_\eta\cdot x$ is negative semidefinite can also be fulfilled for all η small enough.

The solution u_η to the Helmholtz problem with diffusion coefficient a_η (and sesquilinear form B_η) satisfies, according to the previous proposition,

$$\|u_\eta\|_{1,k,G} \lesssim \left(k^3\|f\|_{G\setminus\overline{\Omega}} + k^2\|f\|_\Omega + k^{3/2}\|g\|_{\partial G}\right).$$

$u - u_\eta$ satisfies $B_\eta(u-u_\eta, v) = \int_G (a_\eta - a)\nabla u\cdot\nabla v^*$ for all $v \in H^1(G)$. As the inf-sup-constant of B_η is bounded below by k^{-4}, this gives

$$\|u-u_\eta\|_{1,k,G} \lesssim k^4\|(a_\eta - a)\nabla u\|_G.$$

By the Hölder inequality, we have $\|(a_\eta - a)\nabla u\|_G \lesssim \|a_\eta - a\|_{L^p}\|\nabla u\|_{L^q}$ for all p, q with $1/p + 1/q = 1/2$. Now choose q such that $L^q \subset H^s$ for some $s \in (0, 1/2]$ (e.g., $q = p = 4$ or $q = 8/3$, $p = 8$). Because of $\|a_\eta - a\|_{L^p} \leq \eta$ and the estimate for the H^s-norm of u (see Proposition 3.7), we get

$$\|u - u_\eta\|_{1,k,G} \lesssim k^4\eta(k\|u\|_{1,k,G} + \|f\|_G + \|g\|_{H^{1/2}(\partial G)}).$$

Now choose $\eta = O(k^{-5})$ small enough. By the triangle inequality we finally obtain

$$\begin{aligned}\|u\|_{1,k,G} &\leq \|u - u_\eta\|_{1,k,G} + \|u_\eta\|_{1,k,G}\\ &\lesssim \frac{1}{2}\|u\|_{1,k,G} + k^{-1}(\|f\|_G + \|g\|_{H^{1/2}(\partial G)})\\ &\quad + \left(k^3\|f\|_{G\setminus\overline{\Omega}} + k^2\|f\|_\Omega + k^{3/2}\|g\|_{\partial G}\right),\end{aligned}$$

which gives the claim. ◻

6.3. Proof of the quasi-optimality of the HMM. In this section we give the proof of our central result, namely, Theorem 5.1.

Proof of Theorem 5.1. *Proof of the discrete inf-sup constant* (5.3)*:* Let $\mathbf{v}_{H,h} := (v_H, v_{h,1}, v_{h,2}) \in \mathbf{V}_{H,h}$ be given and let $\mathbf{z} := (z, z_1, z_2) \in \mathcal{H}$ solve

$$\mathcal{B}(\boldsymbol{\psi}, \mathbf{z}) = 2k^2\int_G\int_Y (\psi + \chi_D\psi_2)(v_H^* + \chi_D v_{h,2}^*)\, dydx \qquad \forall\boldsymbol{\psi} := (\psi, \psi_1, \psi_2) \in \mathcal{H}.$$

Due to the regularity of the cell problems (Proposition 3.7), Assumption 3.8 on the stability, and the resulting estimates from Proposition 3.10 it holds that

$$\begin{aligned}\|\mathbf{z}\|_e &\leq 2C_{\mathrm{stab},e}k^{q+1}\|\mathbf{v}_{H,h}\|_e,\\ \|z\|_{H^{1+s_0}_{pw}(G)} &\leq 2C_{\mathrm{reg},0}k^{q+2}\|\mathbf{v}_{H,h}\|_e,\\ \|z_1\|_{L^2(\Omega;H^{1+s_1}(Y^*))} &\leq C_{\mathrm{reg},1}\|\mathbf{z}\|_e \leq 2C_{\mathrm{reg},1}C_{\mathrm{stab},e}k^{q+1}\|\mathbf{v}_{H,h}\|_e,\\ \|z_2\|_{L^2(\Omega;H^{1+s_2}(D))} &\leq C_{\mathrm{reg},2}k\|\mathbf{z}\|_e \leq 2C_{\mathrm{reg},2}C_{\mathrm{stab},e}k^{q+2}\|\mathbf{v}_{H,h}\|_e.\end{aligned} \tag{6.3}$$

Due to (5.1) we can choose $\mathbf{z}_{H,h} := (z_H, z_{h,1}, z_{h,2}) \in \mathbf{V}_{H,h}$ such that

$$\begin{aligned}\|\mathbf{z} - \mathbf{z}_{H,h}\|_e &\leq C_{\mathrm{appr}}\big(H^{s_0}(1 + kH)\|z\|_{H^{1+s_0}_{pw}(G)} + h^{s_1}\|z_1\|_{L^2(\Omega;H^{1+s_1}(Y^*))}\\ &\qquad + h^{s_2}(1 + kh)\|z_2\|_{L^2(\Omega;H^{1+s_2}(D))}\big)\\ &\overset{(6.3)}{\leq} 2C_{\mathrm{appr}}\big(C_{\mathrm{reg},0}k^{q+2}H^{s_0}(1 + kH) + C_{\mathrm{reg},1}C_{\mathrm{stab},e}k^{q+1}h^{s_1}\\ &\qquad + C_{\mathrm{reg},2}C_{\mathrm{stab},e}k^{q+2}h^{s_2}(1 + kh)\big)\|\mathbf{v}_{H,h}\|_e.\end{aligned} \tag{6.4}$$

With this $\mathbf{z}_{H,h}$ we obtain

$$\begin{aligned}\operatorname{Re}\mathcal{B}(\mathbf{v}_{H,h}, \mathbf{v}_{H,h} + \mathbf{z}_{H,h}) &= \operatorname{Re}\mathcal{B}(\mathbf{v}_{H,h}, \mathbf{v}_{H,h} + \mathbf{z} - \mathbf{z} + \mathbf{z}_{H,h})\\ &= \operatorname{Re}\mathcal{B}(\mathbf{v}_{H,h}, \mathbf{v}_{H,h} + \mathbf{z}) - \operatorname{Re}\mathcal{B}(\mathbf{v}_{H,h}, \mathbf{z} - \mathbf{z}_{H,h})\\ &\geq C_{\min}\|\mathbf{v}_{H,h}\|_e^2 - C_B\|\mathbf{v}_{H,h}\|_e\,\|\mathbf{z} - \mathbf{z}_{H,h}\|_e.\end{aligned}$$

Inserting (6.4), we obtain

$$\begin{aligned}
&\operatorname{Re}\mathcal{B}(\mathbf{v}_{H,h}, \mathbf{v}_{H,h} + \mathbf{z}_{H,h}) \\
&\quad\geq C_{\min}\Big(1 - \frac{2C_B C_{\mathrm{appr}}}{C_{\min}}(C_{\mathrm{reg},0}k^{q+2}H^{s_0}(1+kH) + C_{\mathrm{reg},2}C_{\mathrm{stab},e}k^{q+2}h^{s_2}(1+kh) \\
&\qquad\qquad + C_{\mathrm{reg},1}C_{\mathrm{stab},e}k^{q+1}h^{s_1})\Big)\|\mathbf{v}_{H,h}\|_e^2.
\end{aligned}$$

Hence, under the resolution conditions (5.2), this gives $\operatorname{Re}\mathcal{B}(\mathbf{v}_{H,h}, \mathbf{v}_{H,h} + \mathbf{z}_{H,h}) \geq \frac{1}{2}C_{\min}\|\mathbf{v}_{H,h}\|_e^2$. Finally, observing that

$$\begin{aligned}
&\|\mathbf{v}_{H,h} + \mathbf{z}_{H,h}\|_e \\
&\quad\leq \|\mathbf{v}_{H,h}\|_e + \|\mathbf{z}\|_e + \|\mathbf{z} - \mathbf{z}_{H,h}\|_e \\
&\quad\leq \big(1 + 2C_{\mathrm{stab},e}k^{q+1} + 2C_{\mathrm{appr}}(C_{\mathrm{reg},0}k^{q+2}H^{s_0}(1+kH) + C_{\mathrm{reg},1}C_{\mathrm{stab},e}k^{q+1}h^{s_1} \\
&\qquad\qquad + C_{\mathrm{reg},2}C_{\mathrm{stab},e}k^{q+2}h^{s_2}(1+kh))\big)\|\mathbf{v}_{H,h}\|_e \\
&\quad\overset{(5.2)}{\leq} \left(1 + 2C_{\mathrm{stab},e}k^{q+1} + \frac{C_{\min}}{2C_B}\right)\|\mathbf{v}_{H,h}\|_e \\
&\quad\leq \left(k_0^{-(q+1)}\left(1 + \frac{C_{\min}}{2C_B}\right) + 2C_{\mathrm{stab},e}\right)k^{q+1}\|\mathbf{v}_{H,h}\|_e
\end{aligned}$$

finishes the proof of the inf-sup condition.

Proof of the quasi-optimality (5.4)*:* Consider the following (auxiliary) dual problem for $\mathbf{z} := (z, z_1, z_2) \in \mathcal{H}$,

$$\mathcal{B}(\boldsymbol{\psi}, \mathbf{z}) = k^2 \int_G \int_Y (\psi + \chi_D \psi_2)(e_0^* + \chi_D e_2^*)\, dydx \qquad \forall \boldsymbol{\psi} := (\psi, \psi_1, \psi_2) \in \mathcal{H}.$$

As already argued in the proof of the discrete inf-sup constant, $z \in H^{1+s_0}_{pw}(G)$ fulfills the estimate $\|z\|_{H^{1+s_0}_{pw}} \leq C_{\mathrm{reg},0}k^{q+2}\|(e_0, e_1, e_2)\|_e$ due to Proposition 3.10. For all $\mathbf{z}_{H,h} \in \mathbf{V}_{H,h}$, the standard Galerkin orthogonality gives

$$k^2\|e_0 + \chi_D e_2\|^2_{L^2(G\times Y)} = \mathcal{B}(\mathbf{e}, \mathbf{z}) = \mathcal{B}(\mathbf{e}, \mathbf{z} - \mathbf{z}_{H,h}).$$

The continuity of $\mathcal{B}$ w.r.t. the energy norm and an approximation argument like (6.4) yield

$$\begin{aligned}
k^2\|e + \chi_D e_2\|^2_{L^2(G\times Y)} &\leq C_B\|(e_0, e_1, e_2)\|_e\,\|\mathbf{z} - \mathbf{z}_{H,h}\|_e \\
&\leq C_B C_{\mathrm{appr}}\big(C_{\mathrm{reg},0}k^{q+2}H^{s_0}(1+kH) + C_{\mathrm{reg},1}C_{\mathrm{stab},e}k^{q+1}h^{s_1} \\
&\qquad + C_{\mathrm{reg},2}C_{\mathrm{stab},e}k^{q+2}h^{s_2}(1+kh)\big)\|(e_0, e_1, e_2)\|_e^2.
\end{aligned}$$

With the Gårding inequality, we get for any $\mathbf{z}_{H,h} \in \mathbf{V}_{H,h}$

$$\begin{aligned}
\|(e_0, e_1, e_2)\|_e^2 &\leq C_{\min}^{-1}\big(\operatorname{Re}\mathcal{B}(\mathbf{e}, \mathbf{e}) + 2k^2\|e_0 + \chi_D e_2\|^2_{L^2(G\times Y)}\big) \\
&= \operatorname{Re}\big(\mathcal{B}(\mathbf{e}, \mathbf{u} - \mathbf{z}_{H,h}) + 2k^2\|e_0 + \chi_D e_2\|^2_{L^2(G\times Y)}\big) \\
&\leq \frac{C_B}{C_{\min}}\|\mathbf{u} - \mathbf{z}_{H,h}\|_e\,\|(e_0, e_1, e_2)\|_e \\
&\quad + \frac{2C_B C_{\mathrm{appr}}}{C_{\min}}\big(C_{\mathrm{reg},0}k^{q+2}H^{s_0}(1+kH) + C_{\mathrm{reg},1}C_{\mathrm{stab},e}k^{q+1}h^{s_1} \\
&\qquad + C_{\mathrm{reg},2}C_{\mathrm{stab},e}k^{q+2}h^{s_2}(1+kh)\big)\|(e_0, e_1, e_2)\|_e^2.
\end{aligned}$$

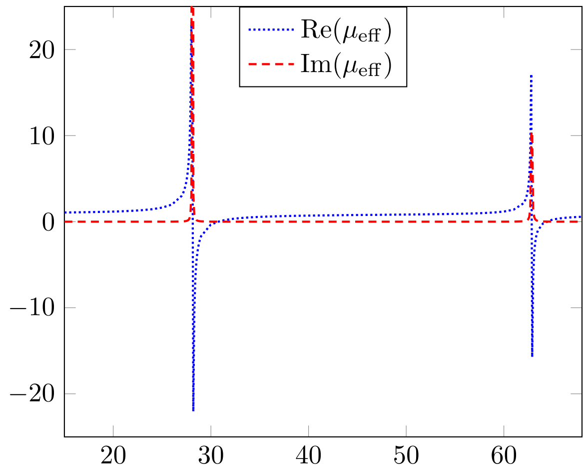

FIG. 2. *Real and imaginary parts of μ_{eff} for changing wavenumber k.*

Together with the resolution conditions (5.2) this gives

$$\|(e_0, e_1, e_2)\|_e^2 \leq \frac{C_B}{C_{\min}} \|\mathbf{u} - \mathbf{z}_{H,h}\|_e \|(e_0, e_1, e_2)\| + \frac{1}{2} \|(e_0, e_1, e_2)\|_e^2$$

and, hence, the first inequality of (5.4). The second inequality directly follows from the approximation properties (5.1) and the regularity estimates from Propositions 3.7 and 3.10. ∎

7. Numerical experiment. In this section we analyze the HMM numerically with particular respect to the convergence order (see Theorem 5.1), the resolution condition (see (5.2)) and the behavior of solutions for different wavenumbers k and different values of μ_{eff}. The implementation was done with the module dune-gdt [53] of the DUNE software framework [6, 7].

We consider the macroscopic domain $G = (0.25, 0.75)^2$ with embedded scatterer $\Omega = (0.375, 0.625)^2$. The boundary condition g is computed as $g = \nabla u_{inc} \cdot n - iku_{inc}$ from the (left-going) incoming plane wave $u_{inc} = \exp(-ikx_1)$. The unit square Y has the inclusion $D = (0.25, 0.75)^2$ and the inverse permittivities are given as $\varepsilon_e^{-1} = 10$ and $\varepsilon_i^{-1} = 10 - 0.01i$. Obviously, the real parts of both parameters are of the same order and, moreover, ε_i is only slightly dissipative.

As the inclusion D is quadratic, the eigenvalues of the Dirichlet Laplacian are explicitly known. Only the eigenvalues where the associated eigenfunctions have nonzero mean contribute to the expansion of μ_{eff}. For our setup, the first interesting values are at $k \approx 28.1$ and $k \approx 62.8$. We compute μ_{eff} using cell problem (3.5) with a grid consisting of 32768 elements on D. Figure 2 shows the behavior of the real and the imaginary part. As predicted, we can see a significant change of behavior around the Laplace eigenvalues, where the real part changes sign and also the imaginary part has large values. Note that for this example, we do not see a dependence of $\text{Im}(\mu_{\text{eff}})$ like k^{-2}, as proved in Proposition 3.5.

In order to analyze the resolution condition, we use a reference homogenized solution by computing the effective parameters with 524288 entities on Y and then solving the effective homogenized equation on G with the same number of entities.

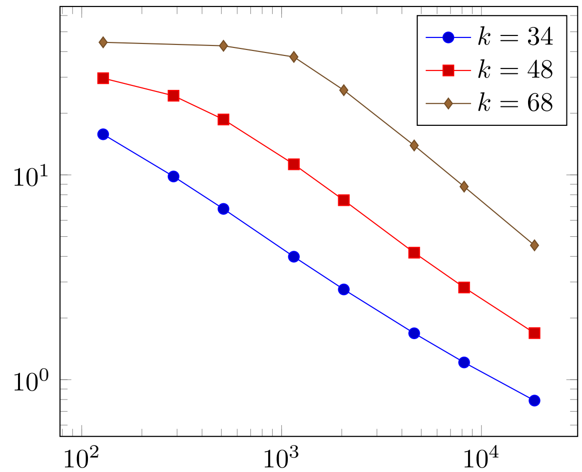

FIG. 3. *Error between homogenized reference solution and macroscopic part u_H of the HMM approximation in weighted H^1-norm versus number of grid entities for different wavenumbers k.*

TABLE 1
Convergence history and EOC for the error between the macroscopic part u_H of the HMM approximation and the reference homogenized solution in the L^2-norm and k-weighted H^1-norm.

$H = 2h$	$\|e_0\|_{L^2(G)}$	$\|e_0\|_{1,k,G}$	EOC($\|e_0\|_{L^2}$)	EOC($\|e_0\|_{1,k}$)
$\sqrt{2} \times 1/8$	0.270474	11.7804630632	—	—
$\sqrt{2} \times 1/12$	0.197617	8.9454269415	0.7740374081	0.678973445
$\sqrt{2} \times 1/16$	0.110372	5.373206314	2.0247154456	1.7718088298
$\sqrt{2} \times 1/24$	0.0513966	2.9702496635	1.2792537865	1.4619724025
$\sqrt{2} \times 1/32$	0.0296714	2.0192725797	1.9097067775	1.3414415096
$\sqrt{2} \times 1/48$	0.0135056	1.2358350102	1.9411761676	1.2109315066
$\sqrt{2} \times 1/64$	0.00767201	0.8863106904	1.9658012347	1.1555624022

We compare the macroscopic part u_H of our HMM approximation with this reference solution in the weighted H^1-norm $\|\cdot\|_{1,k,G}$ for a sequence of simultaneously refined macro- and fine-scale meshes and three different wavenumbers $k = 34$, $k = 48$, $k = 68$; see Figure 3. Note that these wavenumbers are all away from any resonant behavior of μ_{eff}. For higher wavenumbers, finer meshes are needed to obtain convergence: Whereas for $k = 34$, the error convergences for all considered grids, the threshold value for $k = 68 \approx \sqrt{2} \times 34$ is 288 entities; and for $k = 68 = 2 \times 34$, it is 1152 entities. This indicates a resolution condition of $k^2(H + h)$ small in practice, which is standard for continuous Galerkin discretizations of Helmholtz problems.

We now take a closer look at the convergence of the errors and verify the predictions of Theorem 5.1. We choose the wavenumber $k = 29$, which corresponds to $\mathrm{Re}(\mu_{\text{eff}}) < 0$ and thus is also interesting from a physical point of view. Table 1 shows the error between the macroscopic part u_H of the HMM approximation and the reference homogenized solution (as before) in the k-weighted $H^1(G)$-norm and the $L^2(G)$-norm. The experimental order of convergence (EOC), defined as $\mathrm{EOC}(e) := \ln(\frac{e_{H_1}}{e_{H_2}})/\ln(\frac{H_1}{H_2})$, verifies the linear convergence in the H^1-norm predicted theoretically in Theorem 5.1, and the quadratic convergence in the L^2-norm discussed

Table 2

$L^2(G)$-norm of the error to the reference heterogeneous solution for macroscopic part u_H and zeroth order reconstruction u^0_{HMM}.

$H = 2h$	$\|u_\delta - u_H\|_{L^2(G)}$	$\|u_\delta - u^0_{\mathrm{HMM}}\|_{L^2(G)}$	$\mathrm{EOC}(u_\delta - u^0_{\mathrm{HMM}})$
$\sqrt{2} \times 1/8$	0.418463	0.565853	—
$\sqrt{2} \times 1/16$	0.351655	0.174724	1.695349522
$\sqrt{2} \times 1/24$	0.34595	0.0619639	2.5567073663
$\sqrt{2} \times 1/32$	0.346266	0.0340908	2.0770303799
$\sqrt{2} \times 1/48$	0.34733	0.0272449	0.5528495573
$\sqrt{2} \times 1/64$	0.347862	0.0297642	−0.3074226373

afterwards. Note that from the geometry one might expect a reduced regularity of the analytical solution and therefore, a sublinear convergence of the H^1-error. We believe that the linear convergence observed in the experiment does not imply a suboptimality of the error bound in Theorem 5.1, but that in fact, the analytical solution in this special case has full $H^2_{pw}(G)$ regularity, probably because of the boundary condition. This clearly shows that our general theory holds for all regimes of wavenumbers even if they result in unusual effective parameters. However, we observe a small preasymptotic effect for coarse meshes, which indicates that the resolution condition may be stricter for those resonant settings.

Furthermore, we compare the HMM approximation with a detailed reference solution of the heterogeneous problem for $\delta = 1/32$, solved on a fine grid with 524288 entities. Table 2 compares the error to the reference solution for the macroscopic part u_H of the HMM approximation and to the zeroth order L^2-approximation $u^0_{\mathrm{HMM}} = u_H + u_{h,2}(\cdot, \frac{\cdot}{\delta})$. Whereas the error stagnates for u_H, we almost recover the quadratic convergence for u^0_{HMM} with a saturation effect for fine meshes where we enter the regime of the homogenization error. This clearly underlines the necessity of the correctors in the HMM to faithfully approximate the true solution. Note that we do not have results on the homogenization error: We expect strong convergence of u_δ to u^0_{HMM} in the L^2-norm according to [2], but the proof is not applicable to the Helmholtz case.

Finally, we compare two wavenumbers with very different physical meaning: $k = 38$ corresponds to normal transmission, whereas $k = 29$ has $\mathrm{Re}(\mu_{\mathrm{eff}}) < 0$ and thus corresponds to a wavenumber in the band gap where propagation inside the scatterer is forbidden. We consider the macroscopic part u_H of the HMM approximation (with $H = 2h = \sqrt{2} \times 1/64$) and the zeroth order reconstruction u^0_{HMM} (plotted on a well-resolved mesh with 524288 entities) and depict both functions on the whole two-dimensional domain as well as over the line $y = 0.545$, which cuts through a row of inclusions. For $k = 38$, wave propagation with low speed takes place inside the scatterer; see the macroscopic part u_H depicted in Figures 4(a) and 4(b). In contrast to that, we see the expected exponential decay of the wave inside the scatterer for $k = 29$; see the macroscopic part u_H depicted in Figures 5(a) and 5(b). The zeroth order reconstruction u^0_{HMM} can explain this behavior by approximating the heterogeneous solution also inside the inclusion. For $k = 38$, the amplitudes inside the inclusions are as high as the amplitude of the incoming wave; see Figures 4(c) and 4(d). However, we observe very high amplitudes inside the inclusions for $k = 29$; see Figures 5(c) and 5(d). These are caused by eigen resonances incited inside the inclusions. Moreover, these incited waves from neighboring inclusions in-

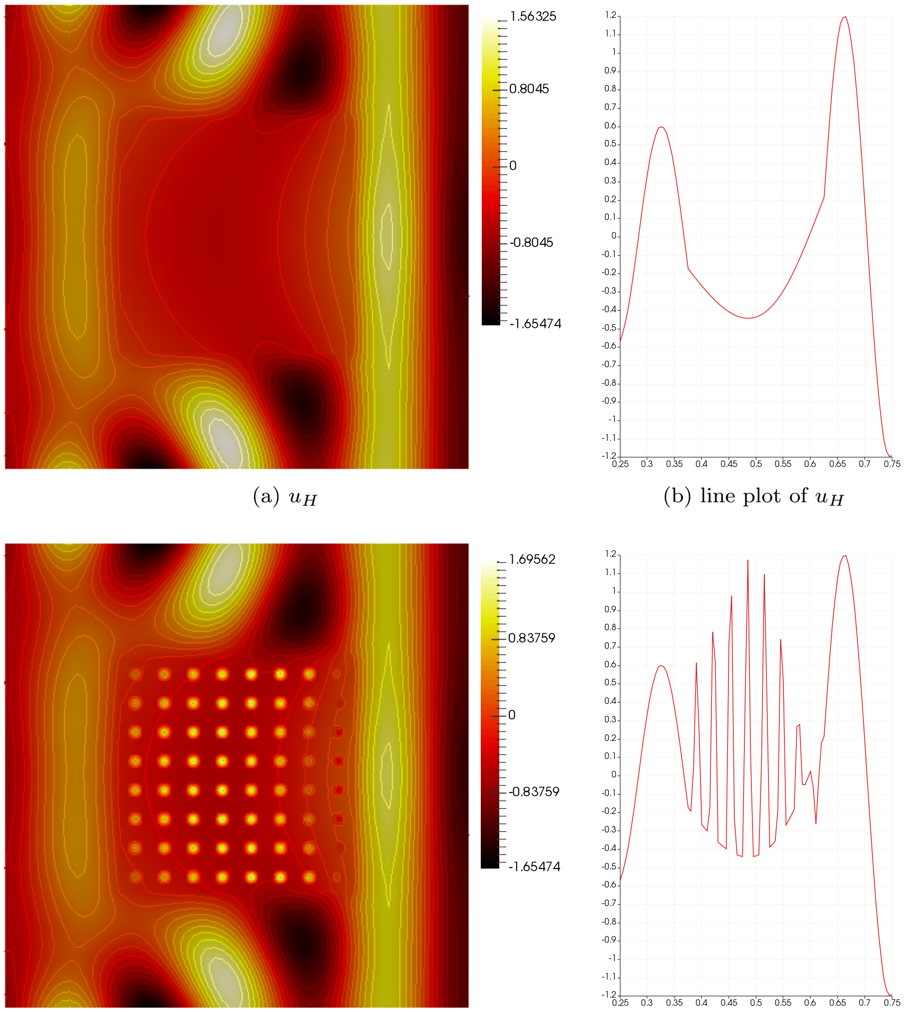

(a) u_H (b) line plot of u_H

(c) u^0_{HMM} (d) line plot of u^0_{HMM}

FIG. 4. *For $k = 38$: Real part of the macroscopic part u_H and real part of zeroth order reconstruction u^0_{HMM}, both on the whole domain (left column) and over the line $y = 0.545$ (right column). Computed with $H = 2h = \sqrt{2} \times 1/64$; u_H visualized on that grid, u^0_{HMM} on fine reference mesh.*

terfere destructively with each other so that over the whole scatterer, no wave can propagate.

Conclusion. We suggested a new HMM for the Helmholtz equation with high contrast. The stability and regularity of the associated analytical two-scale solution is rigorously analyzed and, thereby, a new stability estimate for Helmholtz equations with piecewise constant coefficients is developed. The HMM is defined as direct finite element discretization of the two-scale equation, which is crucial for the numerical analysis. Quasi-optimality of the HMM under the (unavoidable) resolution condition $k^{q+2}(H + h)$ is sufficiently small is proved, where q denotes the exponent for k in the stability estimate. Numerical experiments verify the developed convergence results and analyze the resolution condition. Moreover, the approximation to the heterogeneous solution, obtained from the HMM, explains the effect of evanescent waves in

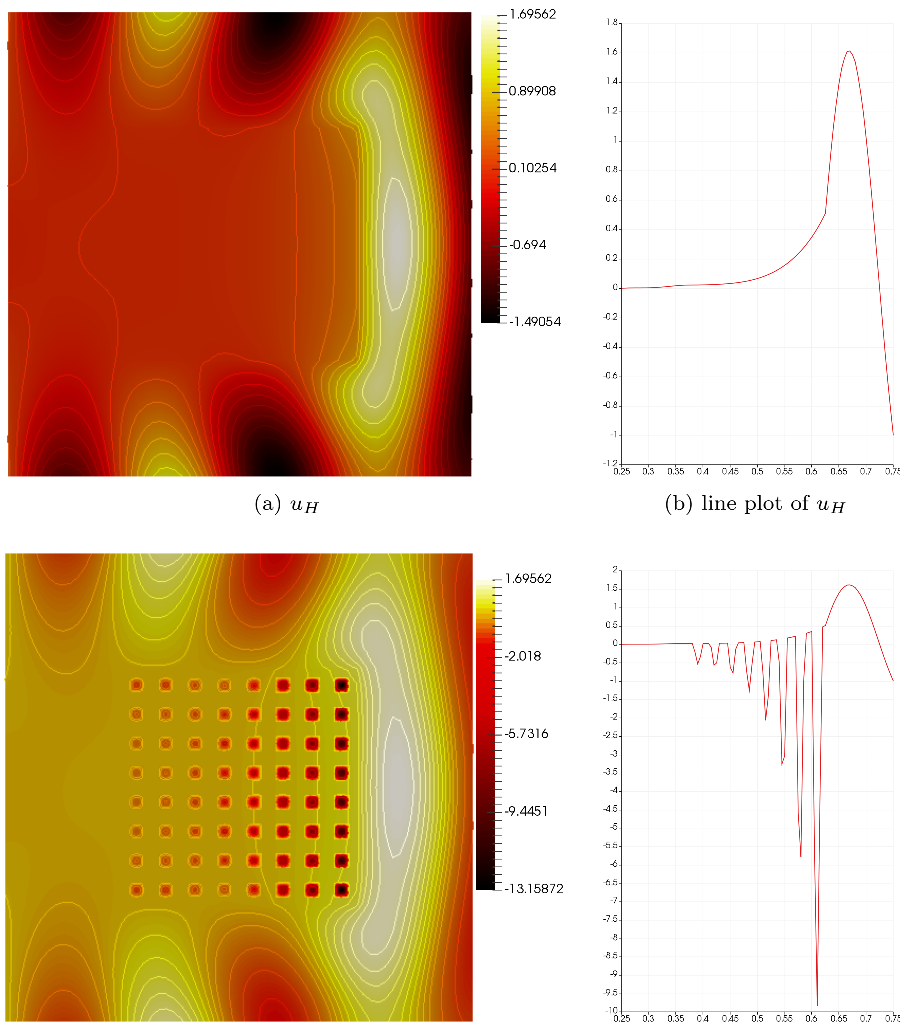

(a) u_H (b) line plot of u_H

(c) u^0_{HMM} (d) line plot of u^0_{HMM}

FIG. 5. *For $k = 29$: Real part of the macroscopic part u_H and real part of zeroth order reconstruction u^0_{HMM}, both on the whole domain (left column) and over the line $y = 0.545$ (right column). Computed with $H = 2h = \sqrt{2} \times 1/64$; u_H visualized on that grid, u^0_{HMM} on fine reference mesh.*

frequency band gaps as destructive interference of eigen resonant waves inside the inclusions.

Acknowledgments. The authors would like to thank P. Henning, A. Lamacz, and B. Schweizer for fruitful discussions on the subject. We also thank the anonymous referees for their valuable remarks.

REFERENCES

[1] A. Abdulle, *On a priori error analysis of fully discrete heterogeneous multiscale FEM*, Multiscale Model. Simul., 4 (2005), pp. 447–459, https://doi.org/10.1137/040607137.

[2] G. Allaire, *Homogenization and two-scale convergence*, SIAM J. Math. Anal., 23 (1992), pp. 1482–1518, https://doi.org/10.1137/0523084.

[3] I. Babuška, *Error-bounds for finite element method*, Numer. Math., 16 (1971), pp. 322–333, https://doi.org/10.1007/BF02165003.

[4] I. M. Babuška and S. A. Sauter, *Is the pollution effect of the FEM avoidable for the Helmholtz equation considering high wave numbers?*, SIAM J. Numer. Anal., 34 (1997), pp. 2392–2423, https://doi.org/10.1137/S0036142994269186.

[5] D. Baskin, E. A. Spence, and J. Wunsch, *Sharp high-frequency estimates for the Helmholtz equation and applications to boundary integral equations*, SIAM J. Math. Anal., 48 (2016), pp. 229–267, https://doi.org/10.1137/15M102530X.

[6] P. Bastian, M. Blatt, A. Dedner, C. Engwer, R. Klöfkorn, R. Kornhuber, M. Ohlberger, and O. Sander, *A generic grid interface for parallel and adaptive scientific computing. II. Implementation and tests in DUNE*, Computing, 82 (2008), pp. 121–138, https://doi.org/10.1007/s00607-008-0004-9.

[7] P. Bastian, M. Blatt, A. Dedner, C. Engwer, R. Klöfkorn, M. Ohlberger, and O. Sander, *A generic grid interface for parallel and adaptive scientific computing. I. Abstract framework*, Computing, 82 (2008), pp. 103–119, https://doi.org/10.1007/s00607-008-0003-x.

[8] T. Betcke, S. N. Chandler-Wilde, I. G. Graham, S. Langdon, and M. Lindner, *Condition number estimates for combined potential integral operators in acoustics and their boundary element discretisation*, Numer. Methods Partial Differential Equations, 27 (2011), pp. 31–69, https://doi.org/10.1002/num.20643.

[9] A. Bossavit, G. Griso, and B. Miara, *Modelling of periodic electromagnetic structures bianisotropic materials with memory effects*, J. Math. Pures Appl. (9), 84 (2005), pp. 819–850, https://doi.org/10.1016/j.matpur.2004.09.015.

[10] G. Bouchitté, C. Bourel, and D. Felbacq, *Homogenization of the 3D Maxwell system near resonances and artificial magnetism*, C. R. Math. Acad. Sci. Paris, 347 (2009), pp. 571–576, https://doi.org/10.1016/j.crma.2009.02.027.

[11] G. Bouchitté and D. Felbacq, *Homogenization near resonances and artificial magnetism from dielectrics*, C. R. Math. Acad. Sci. Paris, 339 (2004), pp. 377–382, https://doi.org/10.1016/j.crma.2004.06.018.

[12] G. Bouchitté and B. Schweizer, *Homogenization of Maxwell's equations in a split ring geometry*, Multiscale Model. Simul., 8 (2010), pp. 717–750, https://doi.org/10.1137/09074557X.

[13] G. Bouchitté and B. Schweizer, *Plasmonic waves allow perfect transmission through subwavelength metallic gratings*, Netw. Heterog. Media, 8 (2013), pp. 857–878, https://doi.org/10.3934/nhm.2013.8.857.

[14] D. Brown, D. Gallistl, and D. Peterseim, *Multiscale Petrov-Galerkin method for high-frequency heterogeneous Helmholtz equations*, in Meshfree Methods for Partial Differential Equations VIII, M. Griebel and M. A. Schweitzer, eds., Lect. Notes Comput. Sci. Eng. 115, 2017, Springer, Cham, Switzerland, pp. 85–115, https://doi.org/10.1007/978-3-319-51954-8_6.

[15] L.-Q. Cao, J.-Z. Cui, and D.-C. Zhu, *Multiscale asymptotic analysis and numerical simulation for the second order Helmholtz equations with rapidly oscillating coefficients over general convex domains*, SIAM J. Numer. Anal., 40 (2002), pp. 543–577, https://doi.org/10.1137/S0036142900376110.

[16] H. Chen, P. Lu, and X. Xu, *A hybridizable discontinuous Galerkin method for the Helmholtz equation with high wave number*, SIAM J. Numer. Anal., 51 (2013), pp. 2166–2188, https://doi.org/10.1137/120883451.

[17] K. Cherednichenko and S. Cooper, *Homogenization of the system of high-contrast Maxwell equations*, Mathematika, 61 (2015), pp. 475–500, https://doi.org/10.1112/S0025579314000424.

[18] P. Ciarlet, Jr. and C. Stohrer, *Finite-element heterogeneous multiscale method for the Helmholtz equation*, C. R. Math. Acad. Sci. Paris, 352 (2014), pp. 755–760, https://doi.org/10.1016/j.crma.2014.07.006.

[19] W. Dörfler and S. Sauter, *A posteriori error estimation for highly indefinite Helmholtz problems*, Comput. Methods Appl. Math., 13 (2013), pp. 333–347, https://doi.org/10.1515/cmam-2013-0008.

[20] W. E and B. Engquist, *The heterogeneous multiscale methods*, Commun. Math. Sci., 1 (2003), pp. 87–132, http://projecteuclid.org/euclid.cms/1118150402.

[21] W. E and B. Engquist, *The heterogeneous multi-scale method for homogenization problems*, in Multiscale Methods in Science and Engineering, Lect. Notes Comput. Sci. Eng. 44, Springer, Berlin, 2005, pp. 89–110, https://doi.org/10.1007/3-540-26444-2_4.

[22] W. E, P. Ming, and P. Zhang, *Analysis of the heterogeneous multiscale method for elliptic homogenization problems*, J. Amer. Math. Soc., 18 (2005), pp. 121–156, https://doi.org/10.1090/S0894-0347-04-00469-2.

[23] A. Efros and A. Pokrovsky, *Dielectric photonic crystal as medium with negative electric permittivity and magnetic permeability*, Solid State Commun., 129 (2004), pp. 643–647, https://doi.org/10.1016/j.ssc.2003.12.022.

[24] S. Esterhazy and J. M. Melenk, *On stability of discretizations of the Helmholtz equation*, in Numerical Analysis of Multiscale Problems, Lect. Notes Comput. Sci. Eng. 83, Springer, Heidelberg, 2012, pp. 285–324, https://doi.org/10.1007/978-3-642-22061-6_9.

[25] S. Esterhazy and J. M. Melenk, *An analysis of discretizations of the Helmholtz equation in L^2 and in negative norms*, Comput. Math. Appl., 67 (2014), pp. 830–853, https://doi.org/10.1016/j.camwa.2013.10.005.

[26] D. Felbacq and G. Bouchitté, *Homogenization of a set of parallel fibres*, Waves Random Media, 7 (1997), pp. 245–256, https://doi.org/10.1088/0959-7174/7/2/006.

[27] D. Gallistl and D. Peterseim, *Stable multiscale Petrov-Galerkin finite element method for high frequency acoustic scattering*, Comput. Methods Appl. Mech. Engrg., 295 (2015), pp. 1–17, https://doi.org/10.1016/j.cma.2015.06.017.

[28] D. Gilbarg and N. S. Trudinger, *Elliptic Partial Differential Equations of Second Order*, Grundlehren Math. Wiss. 224, Springer, Berlin, 1977.

[29] A. Gloria, *An analytical framework for the numerical homogenization of monotone elliptic operators and quasiconvex energies*, Multiscale Model. Simul., 5 (2006), pp. 996–1043, https://doi.org/10.1137/060649112.

[30] R. Griesmaier and P. Monk, *Error analysis for a hybridizable discontinuous Galerkin method for the Helmholtz equation*, J. Sci. Comput., 49 (2011), pp. 291–310, https://doi.org/10.1007/s10915-011-9460-z.

[31] P. Henning and M. Ohlberger, *Error control and adaptivity for heterogeneous multiscale approximations of nonlinear monotone problems*, Discrete Contin. Dyn. Syst. Ser. S, 8 (2015), pp. 119–150, https://doi.org/10.3934/dcdss.2015.8.119.

[32] P. Henning, M. Ohlberger, and B. Verfürth, *A new heterogeneous multiscale method for time-harmonic Maxwell's equations*, SIAM J. Numer. Anal., 54 (2016), pp. 3493–3522, https://doi.org/10.1137/15M1039225.

[33] U. Hetmaniuk, *Stability estimates for a class of Helmholtz problems*, Commun. Math. Sci., 5 (2007), pp. 665–678, http://projecteuclid.org/euclid.cms/1188405673.

[34] R. Hiptmair, A. Moiola, and I. Perugia, *Plane wave discontinuous Galerkin methods: Exponential convergence of the hp-version*, Found. Comput. Math., 16 (2016), pp. 637–675, https://doi.org/10.1007/s10208-015-9260-1.

[35] R. Hiptmair, A. Moiola, and I. Perugia, *A survey of Trefftz methods for the Helmholtz equation*, in Building Bridges: Connections and Challenges in Modern Approaches to Numerical Partial Differential Equations, G. R. Barrenechea, A. Cangiani, and E. H. Geogoulis, eds., Lect. Notes Comput. Sci. Eng. 114, Springer, Cham, Switzerland, 2016, pp. 237–278.

[36] F. Ihlenburg, *Finite Element Analysis of Acoustic Scattering*, Appl. Math. Sci. 132, Springer, New York, 1998, https://doi.org/10.1007/b98828.

[37] S. Irimie and P. Bouillard, *A residual a posteriori error estimator for the finite element solution of the Helmholtz equation*, Comput. Methods Appl. Mech. Engrg., 190 (2001), pp. 4027–4042, https://doi.org/10.1016/S0045-7825(00)00314-5.

[38] A. Lamacz and B. Schweizer, *A negative index meta-material for Maxwell's equations*, SIAM J. Math. Anal., 48 (2016), pp. 4155–4174, https://doi.org/10.1137/16M1064246.

[39] D. Lukkassen, G. Nguetseng, and P. Wall, *Two-scale convergence*, Int. J. Pure Appl. Math., 2 (2002), pp. 35–86.

[40] C. Luo, S. G. Johnson, J. Joannopolous, and J. Pendry, *All-angle negative refraction without negative effective index*, Phys. Rev. B (3), 65 (2002), 201104(R).

[41] J. M. Melenk, *On Generalized Finite-Element Methods*, Ph.D. thesis, University of Maryland, College Park, MD, 1995.

[42] J. M. Melenk and S. Sauter, *Wavenumber explicit convergence analysis for Galerkin discretizations of the Helmholtz equation*, SIAM J. Numer. Anal., 49 (2011), pp. 1210–1243, https://doi.org/10.1137/090776202.

[43] A. Moiola and E. A. Spence, *Is the Helmholtz equation really sign-indefinite?*, SIAM Rev., 56 (2014), pp. 274–312, https://doi.org/10.1137/120901301.

[44] A. Moiola and E. A. Spence, *Acoustic Transmission Problems: Wavenumber-Explicit Bounds and Resonance-Free Regions*, preprint, https://arxiv.org/abs/1702.00745 (2017).

[45] S. O'Brien and J. B. Pendry, *Photonic band-gap effects and magnetic activity in dielectric composites*, J. Phys. Condens. Matter, 14 (2002), 4035, https://doi.org/10.1088/0953-8984/14/15/317.

[46] M. Ohlberger, *A posteriori error estimates for the heterogeneous multiscale finite element method for elliptic homogenization problems*, Multiscale Model. Simul., 4 (2005), pp. 88–114, https://doi.org/10.1137/040605229.

[47] M. Ohlberger and B. Verfürth, *Localized orthogonal decomposition for two-scale Helmholtz-type problems*, AIMS Math., 2 (2017), pp. 458–478, https://doi.org/10.3934/Math.2017.2.458.

[48] I. Perugia, P. Pietra, and A. Russo, *A plane wave virtual element method for the Helmholtz problem*, ESAIM Math. Model. Numer. Anal., 50 (2016), pp. 783–808, https://doi.org/10.1051/m2an/2015066.

[49] D. Peterseim, *Eliminating the pollution effect in Helmholtz problems by local subscale correction*, Math. Comp., 86 (2017), pp. 1005–1036, https://doi.org/10.1090/mcom/3156.

[50] M. Petzold, *Regularity and Error Estimators for Elliptic Problems with Discontinuous Coefficients*, Ph.D. thesis, Freie Universität Berlin, Berlin, 2010.

[51] A. Pokrovsky and A. Efros, *Diffraction theory and focusing of light by a slab of left-handed material*, Phys. B, 338 (2003), pp. 333–337, https://doi.org/10.1016/j.physb.2003.08.015.

[52] A. H. Schatz, *An observation concerning Ritz-Galerkin methods with indefinite bilinear forms*, Math. Comp., 28 (1974), pp. 959–962, https://doi.org/10.1090/S0025-5718-1974- 0373326-0.

[53] F. Schindler, T. Leibner, R. Milk, and S. Kaulmann, *dune-gdt*: 0RS2016, https://doi.org/10.5281/zenodo.35389 (2016).

[54] V. G. Veselago, *The electrodynamics of substances with simultaneously negative values of ε and μ*, Soviet Physics Uspekhi, 10 (1968), pp. 509–514, https://doi.org/10.1070/PU1968v010n04ABEH003699.